

Conceptual Design Report for a Transportable DUCRETE Spent Fuel Storage Cask System

**J. E. Hopf
Sierra Nuclear Corporation
Scotts Valley, California**

Published August 1995

**Idaho National Engineering Laboratory
Environmental and Life Sciences Products Department
Lockheed Idaho Technologies Company
Idaho Falls, Idaho 83415**

**Prepared for the
U.S. Department of Energy
Assistant Secretary for Environmental Management
Under DOE Idaho Operations Office
Contract DE-AC07-94ID13223**

DISTRIBUTION OF THIS DOCUMENT IS UNLIMITED

MASTER

Conceptual Design Report for a Transportable DUCRETE Spent Fuel Storage Cask System

INEL-95/0167

Prepared by:

James E. Hopf
J. E. Hopf
Sierra Nuclear Corporation

8/16/95
Date

Reviewed and Approved by:

WJ Quapp
William J. Quapp, Project Manager
Depleted Uranium Recycle Project

8/16/95
Date



ABSTRACT

A conceptual design has been developed for a spent fuel dry storage cask that employs depleted uranium concrete (DUCRETE) in place of ordinary concrete. DUCRETE, which uses depleted uranium oxide rocks rather than gravel as the concrete's heavy aggregate, is a more efficient overall radiation shield (gamma and neutron) than either steel or ordinary concrete. Thus, it allows the cask weight and size to be substantially reduced. Also, using DUCRETE as shielding avoids, or at least defers, disposal of the depleted uranium as waste. This report focuses on DUCRETE cask transportation issues. The approach studied involves placing the storage cask into a simple steel transportation overpack. Preliminary analyses were performed to demonstrate the transportation system's ability to meet the structural, thermal, and shielding transportation criteria.

Conservative manual calculations were performed to demonstrate the adequacy of the DUCRETE transportation overpack with respect to structural requirements. Two-dimensional thermal analyses were performed on the system (the DUCRETE storage cask inside the steel overpack) using the ANSYS thermal analysis code. Two-dimensional shielding analyses were performed on the system with the MCNP code. Effects of the fuel axial burnup profile and solar radiation are considered.

The analyses show that the proposed system can meet the transportation structural criteria and can easily meet the transportation shielding criteria. The thermal criteria are not as easy to meet because when the storage cask is placed horizontally in the transportation overpack, the DUCRETE storage cask's ventilation duct becomes an insulating dead air space. The maximum allowable temperature for the DUCRETE, which is not yet known, will be the limiting factor. There is a reasonable probability that heat transfer fins extending through the DUCRETE shield, as well as fins on the outer surface of the transportation overpack, will be required for the DUCRETE cask system to accommodate the anticipated heat loads.

CONTENTS

ABSTRACT	v
1.0 INTRODUCTION	1
1.1 DUCRETE Cask Concept	1
1.2 Advantages of the DUCRETE Cask System	3
1.3 DUCRETE Cask System Performance in Storage Mode	5
1.4 Transportation of the DUCRETE Cask	6
2.0 ASSUMPTIONS AND METHODOLOGY	10
2.1 Radiation and Heat Source Specification	10
2.1.1 Gamma Source	10
2.1.2 Neutron Source	11
2.1.3 Cask Internal Heat Generation	12
2.2 Cask Model Geometry and Materials	13
2.2.1 Model Geometry	13
2.2.2 Cask Model Materials and Densities	16
2.3 Analytical Methodology	18
2.3.1 Shielding Analysis	18
2.3.2 Thermal Analyses	26
2.3.3 Structural Analyses	31
3.0 STRUCTURAL EVALUATION	32
3.1 Transportation Overpack	32
3.1.1 Cask Side 6 in. Puncture Drop Event	33
3.1.2 Cask 30 ft Horizontal Drop	33
3.1.3 Cask 30 ft Drop onto Bottom Corner	36
3.1.4 Cask 30 ft Drop onto Top Corner	38
3.2 DUCRETE Storage Cask	40
3.2.1 DUCRETE Cask Outer Shell Bottom Plate	40
3.2.2 DUCRETE Cask Inner Bottom Plate	43
3.2.3 DUCRETE Cask Inner Shell	46
3.2.4 DUCRETE Cask Outer Shell	48
3.3 Inner Canister	48
4.0 THERMAL EVALUATION	51
4.1 Analyzed Cases	52
4.1.1 Base Case	52
4.1.2 Alternative Cases	53
4.2 ANSYS Thermal Analysis Results	55
4.2.1 ANSYS Results	55
4.2.2 Discussion of Results	55
4.3 Maximum Heat Loads for DUCRETE Cask Systems	57
4.3.1 Estimated Cask Temperatures vs. Heat Load	57
4.3.2 DUCRETE Cask Heat Load Limit Results	59

5.0 SHIELDING EVALUATION	62
5.1 Shielding Analyses Performed	62
5.2 Shielding Analysis Results	63
5.3 Acceptable Storage Cask Peak Surface Dose Rates	65
6.0 ESTIMATED CASK WEIGHT	67
7.0 CONCLUSIONS	69
8.0 REFERENCES	71

Figures

1. Standard ventilated storage cask (VSC) system description	2
2. Horizontal cross section view of the DUCRETE cask and the standard VSC	4
3. Vertical cross section view of the DUCRETE cask transportation system	7
4. Finite height cylinder (R-Z) MCNP gamma model of the DUCRETE cask transportation system	22
5. Slab (1-D) MCNP model of the DUCRETE cask bottom end	23
6. Two-dimensional (R-Z) MCNP neutron model of the DUCRETE cask transportation system	25
7. Infinite cylindrical (1-D) MCNP models (gamma and neutron) of the DUCRETE cask	26
8. ANSYS finite difference model of the DUCRETE cask transportation system	27
9. Puncture drop event—a 6 in. side drop onto a 6 in. diameter post	34
10. Cask side drop event—cask (with impact limiters) is dropped 30 ft onto a hard surface	35
11. Cask bottom corner drop event—the cask system is dropped 30 ft onto its bottom corner on a hard surface	37
12. Cask top corner drop event—the cask is dropped onto its top corner on a hard surface, which creates bending stresses in the overpack top lid	39
13. Normal condition lifting of DUCRETE cask this condition creates bending stresses in the cask outer bottom plate	41
14. Cask top end drop event—cask is dropped 30 ft. onto its top end on a hard surface	44
15. Cask bottom end drop event—cask is dropped 30 ft onto its bottom end on a hard surface	47
16. Cask side drop event	49
17. Allowable cask heat load versus maximum allowed DUCRETE temperature for various DUCRETE region thermal conductivities.	60
18. Allowable cask heat load vs. maximum allowed DUCRETE temperature for a) the base case, b) for the no overpack fins case, c) the cask/overpack gap filled with water case, and d) the electro-polished cask outer shell case.	61

Tables

1. Fuel Region Gamma Source Spectrum.	11
2. Neutron Source Spectrum.	12
3. DUCRETE Cask Model Materials.	17
4. Material Composition of DUCRETE Cask Model Regions Used in Shielding Analyses. .	19
5. Neutron Flux-to-Dose Conversion Factors.	20
6. Gamma Flux-to-Dose Conversion Factors.	21
7. DUCRETE Cask ANSYS Model Parameter Summary.	55
8. Peak Temperatures for DUCRETE Cask System Components	56
9. Comparison of Calculated and Estimated Peak Cask Component Temperatures for a Low Heat Load Cask	59
10. DUCRETE Cask Transportation System Dose Rates	64

Conceptual Design Report for a Transportable DUCRETE Spent Fuel Storage Cask System

1.0 INTRODUCTION

The Department of Energy (DOE) Office of Environmental Restoration and Waste Management is evaluating alternative management strategies for depleted uranium (DU) currently stored throughout the DOE complex. Historically, DU has been maintained as a strategic resource for use as depleted uranium metal, for further enrichment, or for breeder reactor fuel.

One of the proposed alternatives is to use depleted uranium oxide "rocks" as the heavy aggregate in the concrete shielding of spent fuel storage casks. The DU could be employed in these casks over storage periods of several decades. At the end of the storage period, the storage casks (containing the DU) could be transported and buried along with their spent fuel in the repository. If this is not possible, the DU could be buried separately (elsewhere) or used in some other application.

This report covers the transportation portion of the evaluation of a conceptual design for a DU concrete (DUCRETE) storage cask. Analyses are presented that demonstrate the proposed system's ability to meet cask transportation requirements.

1.1 DUCRETE Cask Concept

The DUCRETE spent fuel dry storage cask design concept is based on the Sierra Nuclear Corporation (SNC) Ventilated Storage Cask (VSC) system. The VSC system consists of a steel canister containing the spent fuel inside a concrete storage cask. In the DUCRETE cask design,¹ depleted uranium oxide "rocks" are used in place of gravel as the concrete's coarse aggregate. The DUCRETE cask design also has an outer steel shell to contain the DUCRETE and protect it from normal environmental conditions. Figure 1 shows a view of the standard VSC system, which consists of the inner canister (with a 24 PWR fuel assembly or a 65 BWR fuel assembly basket) and the concrete cask. An annular gap between the canister and the cask allows passive convective cooling of the fuel canister. The cask has a system of inlet and outlet ducts to allow airflow through the annulus. The DUCRETE cask system will have a similar inlet and outlet vent structure, although smaller than that of the VSC cask because of the thinner cask wall.

The VSC and DUCRETE systems will have the same capacity for spent fuel, 24 PWR assemblies or 65 BWR assemblies. The licensed fuel canister for the VSC system, referred to as the Multi-Assembly Sealed Basket (MSB), is similar in dimensions and weight to the proposed Multi-Purpose Canister (MPC) for the DOE's Civilian Radioactive Waste Management System (CRWMS). The standard VSC concrete cask and the DUCRETE cask will be able to accommodate both canisters.

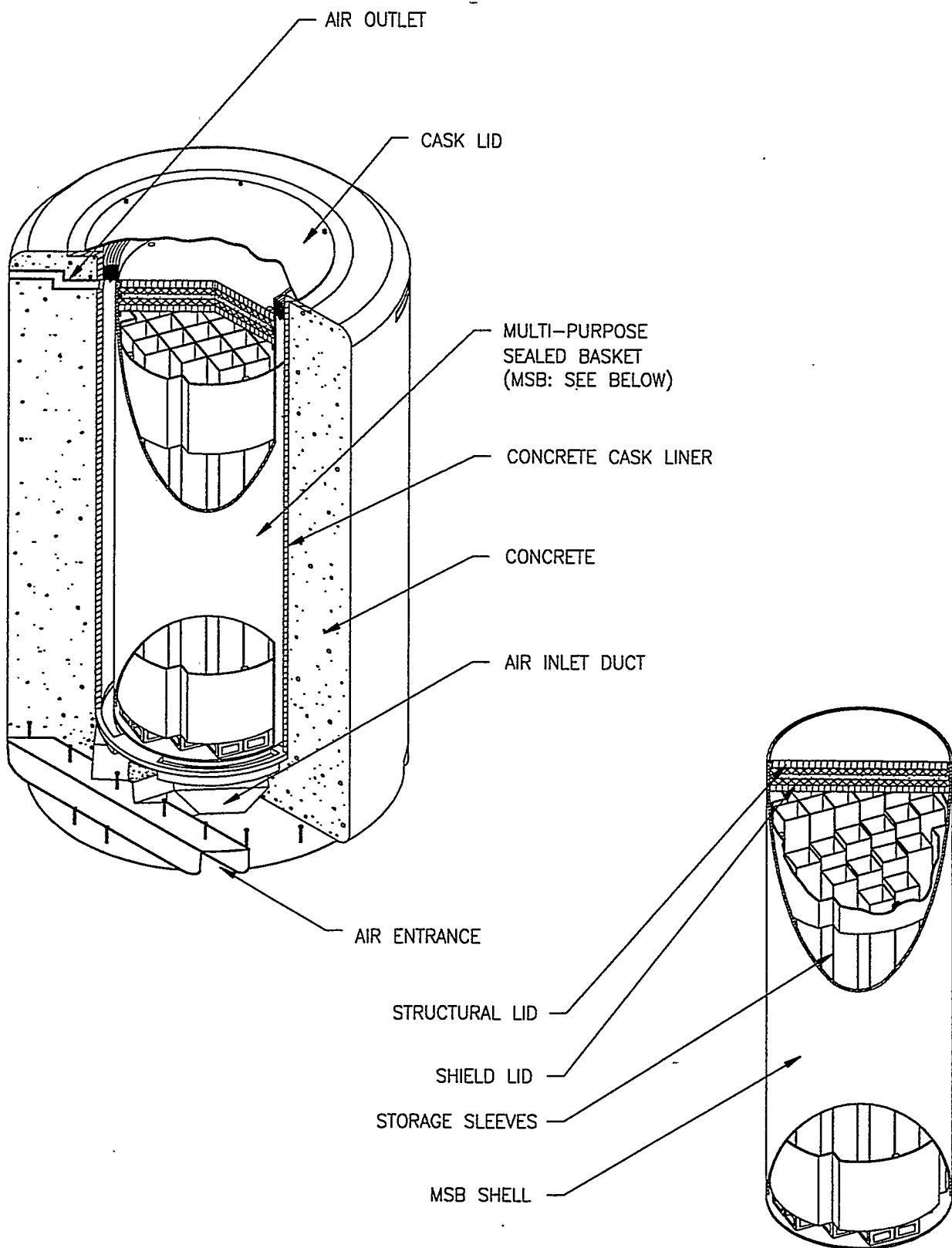


Figure 1. Standard ventilated storage cask (VSC) system description.

1.2 Advantages of the DUCRETE Cask System

DUCRETE is a more effective overall radiation shield for the gamma and neutron sources associated with spent nuclear fuel than any of the standard shielding materials used in spent fuel storage or transportation casks. If a DUCRETE shield of a given thickness is compared to steel, concrete, lead, or uranium shields of the same thickness or weight, the DUCRETE shield will yield the lowest overall dose rate. A concrete shield will yield neutron dose rates similar to the DUCRETE shield, but much higher gamma dose rates. Steel, lead, and uranium shields will yield lower gamma dose rates than a DUCRETE shield, but the neutron dose rates will be so much higher that the total dose rate will be higher than that of the DUCRETE shield. Because DUCRETE is a balanced shielding material, offering comparable shielding effectiveness for both gamma and neutron radiation, the thickness required to yield a given total dose rate is minimized. An additional feature of DUCRETE is that the concentration of uranium oxide pellets can be varied, which allows adjustment of the relative gamma and neutron shielding effectiveness to achieve a minimum total dose rate for a given shield weight.

In addition to replacing gravel with UO_2 rocks as the coarse aggregate, replacing ordinary sand with hydrogen-bearing sand such as colemanite for the fine aggregate is being considered. This will significantly increase the neutron shielding effectiveness of the DUCRETE without significantly affecting the gamma shielding. This would give DUCRETE additional superiority over the other common shielding materials.

Thus replacing the concrete in the standard VSC cask with DUCRETE will allow the size and weight of the cask system to be reduced significantly without allowing unacceptable dose rates on the cask exterior. The thickness of the concrete shield will be reduced from about 2.5 ft to under 1 ft, and the diameter of the DUCRETE cask system will be only about 2/3 that of the standard VSC system (~90 vs. ~135 in.), see Figure 2. Even though DUCRETE is over twice the density of ordinary concrete, the overall weight of the shield will be reduced significantly. The total system weight will fall from over 135 tons to roughly 100 tons.

The reduction in cask system size and weight, along with the metal shell around the DUCRETE cask exterior, will allow a DUCRETE cask containing an inner canister to be placed directly in the spent fuel pool for loading. The loaded DUCRETE cask can then be removed from the pool, decontaminated, and transported directly to the storage pad. A canister transfer cask is not necessary. Thus, cask loading operations are much simpler than those required for present-day concrete storage cask systems. With respect to loading operations, the DUCRETE cask will behave like metal cask systems. Metal casks, however, which employ thick stainless steel shells and additional neutron shielding material, are much more expensive (about three times) than the DUCRETE cask. DUCRETE cask costs are estimated to be similar to those of concrete cask systems.

Another significant benefit of the reduction in storage cask size and weight is that it may be possible to transport the loaded DUCRETE cask--it would basically behave like a "thick-walled" multi-purpose canister. The DUCRETE cask would simply be moved from the storage pad, placed directly in a thin-walled steel transportation overpack, and positioned on a

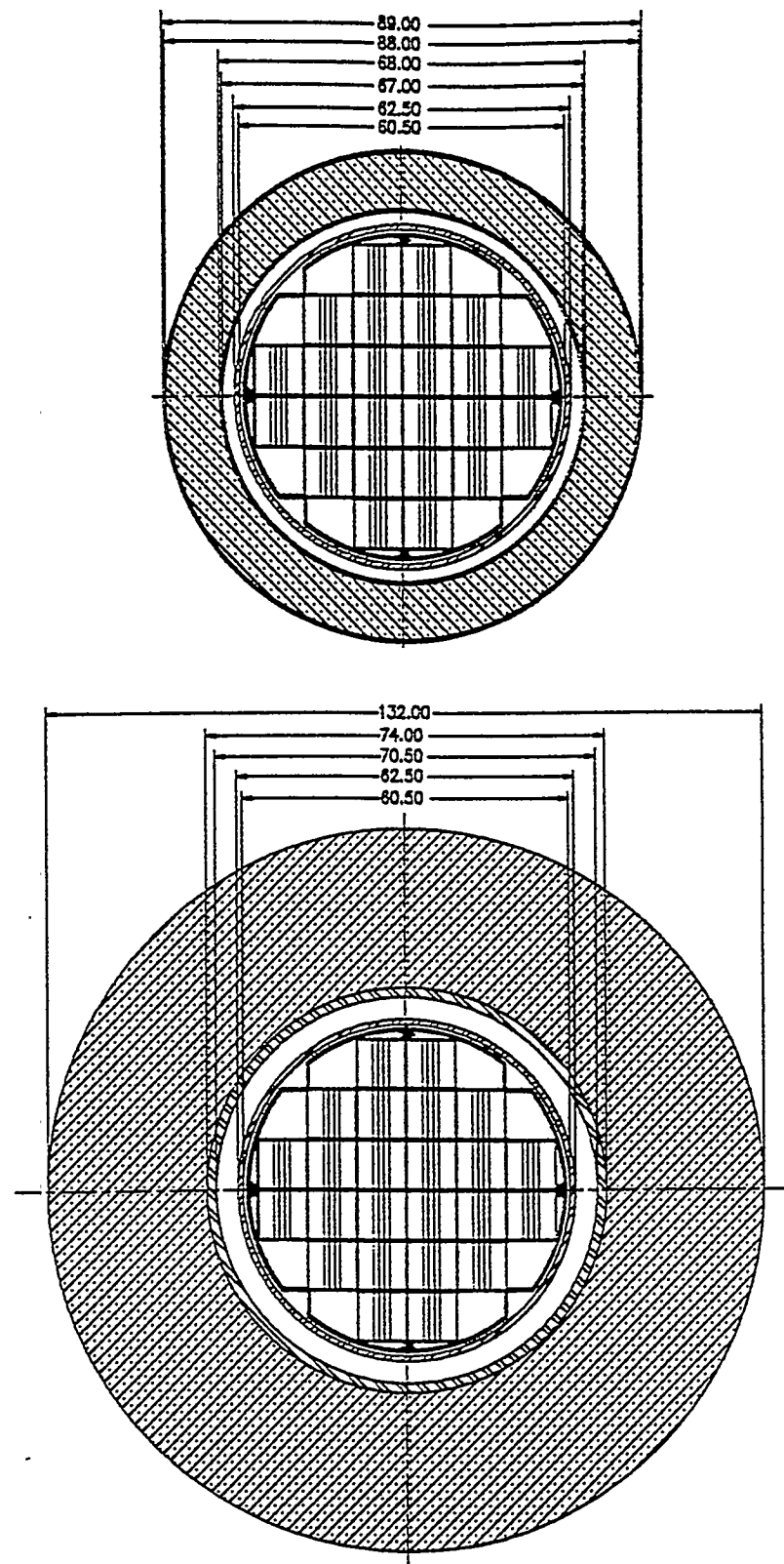


Figure 2. Horizontal cross section view of the DUCRETE cask and the standard VSC.

rail car. It would not be necessary, as in the VSC system, to move the inner canister from the storage cask (using a transfer cask) to an expensive, heavily shielded transportation cask. The DUCRETE cask could be shipped to retrievable storage, where it would merely be taken out of the transportation overpack and placed directly on the storage pad, or it could be shipped to a repository, where the whole cask would be placed in a repository overpack and buried.

The DUCRETE cask system should be able to meet all of the requirements that have been established for the MPC system. Not only can a DUCRETE cask accommodate an MPC, but the entire DUCRETE cask system weight, including a loaded, water-filled MPC, is ~100 tons. This meets the MPC system weight requirement for loaded transfer casks, which the DUCRETE cask is comparable to. Also, the estimated total weight of the transportation overpack, DUCRETE cask, and a dry, loaded MPC is under 125 tons. This meets the MPC system weight requirement for a loaded transportation cask.

1.3 DUCRETE Cask System Performance in Storage Mode

A conceptual design study of the DUCRETE cask system in storage mode was performed by Sierra Nuclear Corp.¹ Shielding analyses estimated peak dose rates on the DUCRETE cask sidewall. (Dose rates on the cask top, which are governed by the top lid of the inner canister, are expected to be the same as for the VSC since both systems use the same inner canister. Detailed analyses had been performed for the licensed VSC system.²) Thermal hydraulic calculations were performed to estimate the effect of reducing the ventilation duct thickness from 4 to 2 in. In storage mode, this duct is responsible for the great majority of the heat removal for the cask systems. Very little of the internal heat is deposited in, and must travel through, the concrete (or DUCRETE) shield region, which lies outside the ventilation duct. Therefore, the nature of the shield region has no significant impact on system temperatures. Finally, the conceptual design report included a qualitative discussion on the performance of the DUCRETE shield in comparison to the concrete shield with respect to many structural issues such as cask drop, tip over, and missile impacts.

In the shielding analyses, several different spent fuel radiation sources and DUCRETE shield compositions were studied. For spent fuel with a burnup level of 35 GWd/MTU and a cooling time of 5 years, the design basis fuel for the standard VSC cask system, peak dose rates on the DUCRETE cask sidewall were estimated to be about 55 mrem/hr for the optimum DUCRETE shield composition. This composition had UO₂ rocks occupying about half of the DUCRETE shield volume and assumed colemanite sand as the fine aggregate. If ordinary sand is used, the peak surface dose rate rises to ~73 mrem/hr.

If the gamma and neutron source descriptions in the MPC system specification are used, the peak surface dose rate rises to ~85 mrem/hr for colemanite sand DUCRETE and ~140 mrem/hr for ordinary sand DUCRETE. The optimum UO₂ volume fraction drops to 42% for colemanite sand DUCRETE and only 33% for ordinary sand DUCRETE. These changes are primarily attributable to the neutron source strength specified for the MPC system, which is a factor of three higher than that of the VSC system's design basis fuel. In DUCRETE, the cement and fine aggregate (in the colemanite sand case) are primarily responsible for the neutron attenuation. Therefore, a higher neutron source strength requires a reduction in the UO₂ (coarse aggregate) volume fraction.

The estimated dose rates for the DUCRETE cask exterior were found to be within the acceptable range. Typical peak surface dose rates for metal cask systems presently licensed and in use are in the 50-100 mrem/hr range for fuels similar to the VSC system design basis fuel. The DUCRETE cask system peak surface dose rates are predicted to be within this range.

The thermal hydraulic analyses¹ show that reducing the ventilation duct thickness from 4 to 2 in. does not significantly affect the performance of the duct. The overall resistance to airflow in the duct increases by ~20%, which causes a 7°F increase in the temperature of the air leaving the duct. Thus, the temperature of the internal canister is only expected to rise by a few degrees. Also, since very little heat flows through the shield, which is outside the ventilation duct, the nature of the shield will have little effect on its temperature. Peak DUCRETE temperatures will be governed by the temperature of the air in the ventilation duct. Therefore, the temperatures throughout the DUCRETE cask system will be very close to those of the standard VSC cask system.

The conceptual design study did not include formal structural analyses for the DUCRETE cask in storage mode because most structural issues pertain to the inner canister and the formal calculations for the VSC system inner canister² (MSB) are applicable. With respect to issues such as cask tip over and missile impacts, it was pointed out¹ that although the DUCRETE shield is much thinner than the VSC system concrete shield, it is also much denser, which aids in the absorption of blows such as missile impacts. The strength of DUCRETE is expected to be similar to that of concrete. Also, the 0.5 in. thick steel outer shell in the DUCRETE cask system will greatly spread out the force of impacts associated with tip overs and missiles. For these reasons, it is thought that the DUCRETE cask system will be at least as resistant to these events as the standard VSC cask system. Structural issues will have to be examined in more detail during the formal design phase of the DUCRETE cask system.

1.4 Transportation of the DUCRETE Cask

The concept for DUCRETE cask transportation is to lift the entire DUCRETE storage cask from the storage pad and place it in a transportation overpack consisting of a 2 in. thick cylindrical shell of stainless steel (XM-19). The overpack will have a thick bottom plate and a thick closure plate of the same material. The closure plate will feature a bolted closure and a recessed lid. A vertical cross section of the DUCRETE cask system inside the transportation overpack is shown in Figure 3. The overpack will support the DUCRETE cask and its canister, reducing any localized loads on their surfaces. The overpack will be required to bear the loaded DUCRETE storage cask and meet all of the transportation structural requirements, such as a 30 ft drop onto an unyielding surface and a 6-in. puncture drop.

The DUCRETE cask system overpack is expected to be much simpler and less expensive than conventional transportation casks, even though the use of a relatively expensive steel (XM-19) was required to meet the structural criteria while remaining within weight limits. This is due to the fact that the DUCRETE system overpack consists of a simple steel shell, whereas standard transportation casks are a much more complicated, multilayered structure. The overpack will have impact limiters, similar to ones used in

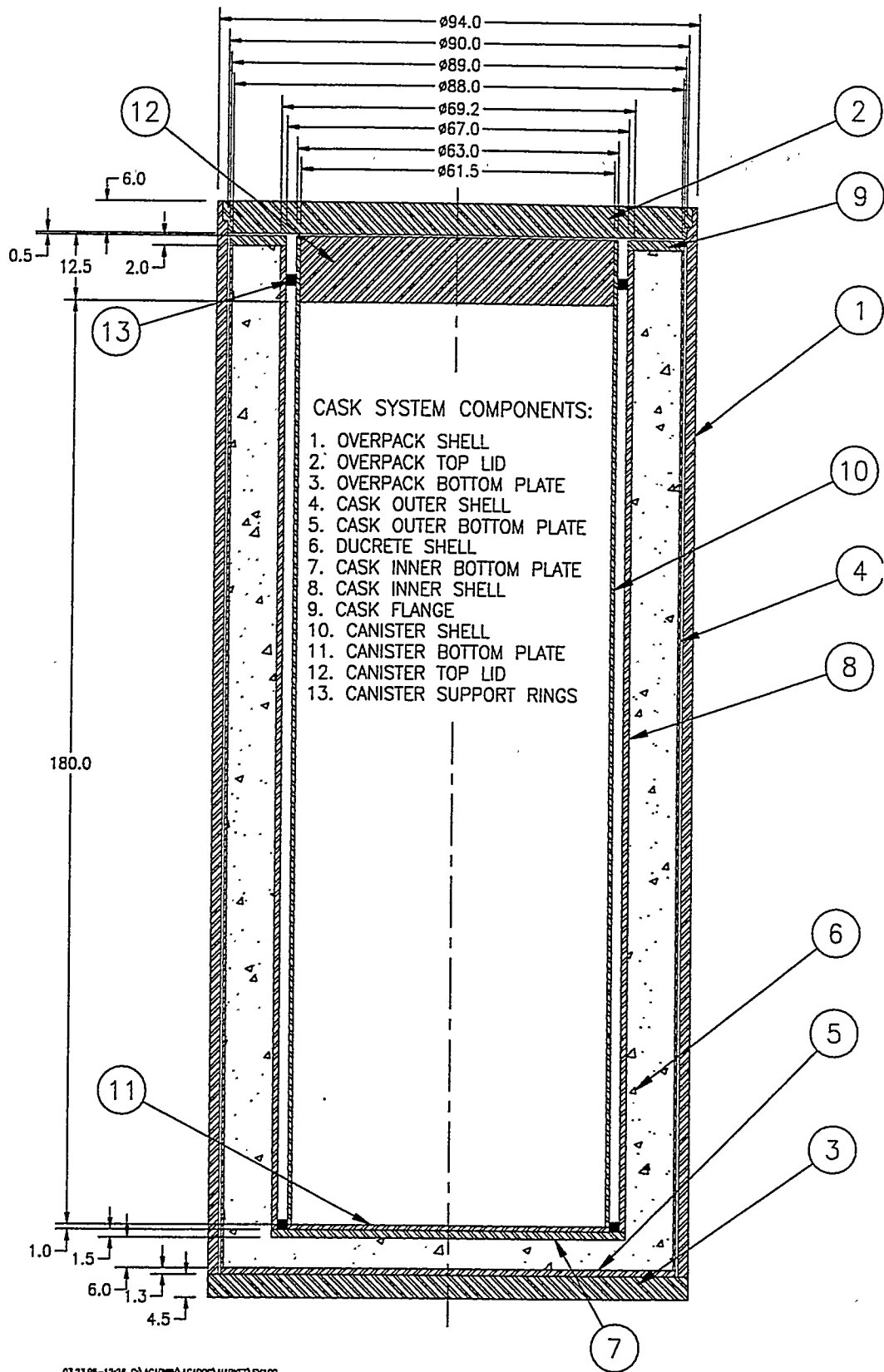


Figure 3. Vertical cross section view of the DUCRETE cask transportation system.

several present day rail cask designs, fastened to the top and bottom ends. A fin structure will probably be employed to enhance heat transfer. The overpack's outer surface will also be covered with a coating (such as white paint) that will minimize the absorption of solar radiation and yield a surface emissivity in excess of 0.9. Because the DUCRETE cask transportation system concept does not involve placing the transportation overpack in the spent fuel pool—the DUCRETE storage cask is lifted directly out of the pool, decontaminated, moved to a storage pad or to a staging area, and at that location placed in the transportation overpack—the overpack design does not have to consider surface decontamination.

With respect to transportation regulations, the overpack will form the containment boundary of the system. The inner canister, with its double welded lid closure, could be considered a second containment boundary.

Some changes in the DUCRETE storage cask design presented in Ref. 1 will be required to meet transportation criteria. The inner shell of the DUCRETE cask will have to be thicker than 0.5 in., particularly on the cask bottom end. Also, a heat transfer fin structure through the DUCRETE material will probably be required. Finally, a design feature for suspending the inner canister in the center of the DUCRETE cask cavity when the system is horizontal will have to be added. None of these changes are expected to have a significant impact on the performance of the DUCRETE cask in storage mode. A thicker cask shell will require replacing some DUCRETE with steel. This will lead to a small increase in dose rates because DUCRETE is a better overall shielding material on a per weight basis. Since the heat transfer fins are expected to occupy ~5% (or less) of the DUCRETE shield volume, they are not expected to significantly affect external dose rates. They may, however, have some effect on the cask weight. Streaming problems are not expected. The structure for suspending the canister in the cask cavity is designed so that it will not have any significant effect on the performance of the ventilation duct while the cask is in storage mode.

For the above reasons, the changes required in the original DUCRETE storage cask design to make it transportable do not alter the storage cask's performance or change any of the basic conclusions reached in Ref. 1.

This report presents analyses demonstrating the DUCRETE cask transportation system's compliance with structural, thermal, and shielding requirements for transportation casks. Since criticality performance is completely governed by the design of the system's inner canister, and the DUCRETE cask system will accommodate the licensed VSC system inner canister as well as the (to be designed) DOE MPC, which are required to meet the criticality criteria, criticality issues are not addressed in this report.

The analyses consider a loaded DUCRETE cask inside the steel transportation overpack. Conservative manual calculations demonstrate the structural adequacy of the cask system. For the thermal and shielding analyses, detailed two-dimensional (R-Z) models of the cask system were developed and analyzed with the industry-standard ANSYS and MCNP codes.

The models assume that the DUCRETE cask system is loaded with an MPC containing the heat and radiation sources given in the MPC system specification. The heat and radiation levels are much higher than those assumed in the VSC system's licensing calculations because the MPC specification is based on fuel with a higher burnup level than the SNC system's design basis fuel. Also, the MPC system canister is estimated to be longer and heavier than the VSC system canister. The DUCRETE cask system will meet the requirements of the DOE MPC system.

With respect to structural considerations, the overpack is simply made strong enough to meet all of the transportation structural requirements. The only structural requirement for the DUCRETE storage cask is that its steel shells be strong enough to support the DUCRETE and hold it in place during the hypothetical transportation cask drop events. Specifically, the DUCRETE cask inner shell is required to keep the DUCRETE material from crushing the inner canister during an accident.

One structural issue that must be addressed is how the inner canister is suspended within the ventilation duct. In storage mode, the inner canister may simply sit (laterally unsupported) inside the DUCRETE storage cask such that there is a 2 in. space around the canister. In transport mode, however, the system is horizontal. Some mechanism or design feature that will support the canister in the center of the cask cavity must be found. A proposed method of suspension is presented in Section 2.2.1.

Thermal considerations are more of a concern. The DUCRETE storage cask relies on a ventilation duct to remove heat from the surface of the inner canister. When the DUCRETE storage cask is placed in the steel overpack, this ventilation is cut off, leaving a 2 in. dead air (or helium) gap around the inner canister. Another 0.5 in. gap exists between the DUCRETE storage cask and the steel overpack. The fins and high emissivity surface of the overpack, however, largely make up for these problems, as the analyses will show. Another thermal issue is the maximum temperature that the DUCRETE material can withstand. The DUCRETE temperature limit will be lower than that of traditional transportation cask materials such as steel or lead. The thermal analyses show that the DUCRETE material temperature limit is the limiting constraint on the heat load that the DUCRETE cask system can accommodate in transport mode.

The transportation overpack also provides a substantial amount of additional shielding. The DUCRETE cask transportation system easily meets the shielding requirements.

2.0 ASSUMPTIONS AND METHODOLOGY

2.1 Radiation and Heat Source Specification

The transportation mode shielding evaluations, presented in Section 5, use the gamma and neutron source descriptions given in the DOE MPC system specification.³ These source terms are conservatively high estimates of the radiation from 40,000 MWd/MTU, 10-year-cooled PWR fuel. These values represent a bounding case since the design basis radiation source terms for all presently licensed storage and transport cask systems (of similar size and capacity) are much lower.

Total cask source strengths are based upon 24 PWR assemblies. The MPC may also hold as many as 52 BWR assemblies. Based upon the specified BWR source strengths, 52 BWR assemblies will produce a total cask neutron source that is ~13% higher than that of 24 PWR assemblies. However, based upon the specified BWR gamma source strengths, 52 BWR assemblies produce a total cask gamma source that is ~12% lower than that of 24 PWR assemblies. Also, the specified BWR gamma source spectrum is somewhat softer than that of PWR fuel. Since gamma dose rates are the greater contributor to the total dose rate for the great majority of the DUCRETE cask systems studied in Ref. 1, the PWR assembly case will generally yield the highest dose rates. Therefore, the PWR source was assumed in the transportation shielding analyses.

2.1.1 Gamma Source

The gamma spectrum given in the MPC system specification³ for use in transportation mode shielding analyses is shown in Table 1. The total gamma source strength, also listed in the specification, is 4.5e+15 gamma/sec-assembly. This corresponds to a total cask gamma source of 1.08e+17 gamma/sec, given the cask payload of 24 PWR assemblies. The MPC system specification lists a peak gamma source strength of 5.4e+15 gamma/sec-assembly, which occurs at the axial center of the PWR assemblies. Thus, the gamma source strength near the axial center is ~20% higher than the assembly average value.

In the two-dimensional (R-Z) MCNP model of the DUCRETE cask system, the gamma radiation emerges from a cylindrical volume that fills the entire inner canister. The source region begins 4 in. above the bottom of the canister cavity, extends upward 144 in., and has a radius of 30.72 in. The shielding analyses model the axial distribution of the gamma source within the fuel assemblies. In these analyses, the axial gamma source distribution is assumed to have a cosine shape. The source region is subdivided (axially) into six 2-ft-high subcylinders. The gamma source strengths for these six regions, relative to the assembly average, from end to end, are 0.75, 1.05, 1.2, 1.2, 1.05, and 0.75. This distribution averages 1.0 and has a peak source strength 1.2 times the average. Also, the distribution roughly follows a cosine distribution.

For the shielding analyses that specifically modeled the cask bottom end, only the bottom half of the cask and source were modeled. Thus, in this model there are three source subregions, the bottom one having a relative source strength of 0.75, the middle one having a

source strength of 1.05, and the top one having a source strength of 1.2. Gammas generated in the top half of the cask will not contribute significantly to cask bottom end dose rates, as they have to travel through more than 6 ft of fuel.

The cask bottom shielding analyses also calculate the gamma dose rate on the cask bottom due to the assembly bottom hardware. The MPC specification gives a Co-60 activation level of 65.6 Ci per assembly bottom nozzle, which is a gamma source of $4.85e+12$ gammas/sec-nozzle and a total cask source of $1.165e+14$ gammas/sec-cask. This gamma source is evenly distributed within the cylindrical region occupying the bottom 4 in. of the canister interior. Note that, based on the source strengths specified for the MPC system, 24 PWR assembly bottom nozzles are a higher total cask gamma source than 52 BWR assemblies.

2.1.2 Neutron Source

The neutron source used in the two-dimensional MCNP shielding models is based upon the data given in the MPC system specification,³ which lists an average PWR assembly neutron source strength of $2.0e+8$ n/sec-assembly and a peak neutron source strength equivalent to $4.4e+8$ n/sec-assembly. This corresponds to a total cask neutron source of $4.8e+9$ n/sec. The neutron source region is identical to the fuel gamma source region and is also broken down into six axial subregions to model the axial distribution in source strength.

Inspection of databases that give neutron source strengths as a function of assembly burnup level and cooling time⁴ shows that neutron source strength is an exponential function of assembly burnup. The assembly burnup profile is approximated as a cosine distribution, so the neutron source strength will have a very different distribution. Looking at the specified peak and average neutron source strengths, it can be seen that no cosine distribution could produce the required peak value without exceeding the listed average value (given that negative source strengths on the ends do not occur).

The neutron source strengths for the six axial subregions were determined as follows. The relative burnup distribution was assumed to equal that of the gamma source strength (0.75, 1.05, 1.2, 1.2, 1.05, 0.75). The logarithms of the neutron source strengths were assumed to have a linear relation with burnup level (as is shown by the databases). It was specified³ that at 40,000 MWd/MTU, the neutron source strength is $2.0e+8$ n/sec-assembly. It

Table 1. Fuel Region Gamma Source Spectrum (MPC Specification for PWR Fuel).

Mean Energy Level (MeV)	Source Strength Fraction
9.0	2.44e-11
7.0	2.13e-10
5.0	1.84e-09
3.5	7.22e-08
2.75	5.82e-07
2.25	8.37e-06
1.75	4.02e-04
1.25	3.88e-02
0.85	3.86e-02
0.575	4.25e-01
0.375	1.14e-02
0.225	2.35e-02
0.125	2.71e-02
0.085	2.87e-02
0.0575	4.86e-02
0.0375	6.31e-02
0.015	5.22e-02
0.010	2.43e-01

is also known that at the assembly peak burnup level of 48,000 MWd/MTU (1.2 x 40,000), the neutron source strength is 4.4e+8 n/sec-assembly (equivalent). The natural logarithms of these two values are 19.114 and 19.902, respectively. These two "data points" define a line that approximates neutron source strength versus burnup level. This formula was used to determine the neutron source strengths at the other two burnup levels, 42,000 MWd/MTU (1.05 x 40,000) and 30,000 MWd/MTU (0.75 x 40,000). The logarithms of these neutron source strengths are 19.311 and 18.129, respectively. These correspond to neutron source strengths of 2.436e+8 and 7.47e+7, respectively. Thus, the neutron source strengths for the three subregion burnup levels are 7.47e+7, 2.436e+8, and 4.4e+8.

Note that these three neutron source strength levels produce an average neutron source strength of 2.53e+8 n/sec-assembly, greater than the average assembly value listed in the MPC specification. This is because the value in the specification is the neutron source strength at the assembly average burnup level, not the assembly average neutron source strength. Due to the very nonlinear dependence of the neutron source strength on the burnup level, the average neutron source strength is significantly greater. This approach is conservative because the analyses use a total assembly neutron source of 2.53e+8 n/sec-assembly, which is 26% higher than the value listed in the specification.

The neutron source spectrum used in the shielding analyses, which also comes from the MPC specification,³ is shown in Table 2.

2.1.3 Cask Internal Heat Generation

The assembly heat generation level assumed in the thermal analyses was 0.73 kW per assembly, the value listed in the MPC specification.³ This corresponds to a cask heat generation rate of 17.52 kW. The heat source region is the same as the neutron and gamma source regions, the entire inner area of the canister.

The axial heat generation profile in the fuel was modeled in the two-dimensional (R-Z) thermal analyses of the cask. The MPC specification lists a peak heat generation rate of 0.94 kW (equivalent). This corresponds to a peaking factor of 1.288. If the relative heat generation rate were to follow the function

$$\frac{H}{H_0} = 0.7854 \cos\left(\frac{\pi z}{144}\right) + 0.5, \quad (1)$$

then the average relative heat over the axial span would be exactly 1.0 and the peak relative heat, in the axial center, would be 1.2854. The relative heat generation at the top and bottom ends of the fuel region would be half the average value. This function agrees with the peak and average values given in the MPC specification very well.

The source region is divided into six axial subregions with relative powers of 0.7, 1.05,

Table 2. Neutron Source Spectrum.

Energy Group (MeV)	Source Strength Fraction
6.43 - 20.0	0.0185
3.0 - 6.43	0.21
1.85 - 3.0	0.234
1.4 - 1.85	0.131
0.9 - 1.4	0.177
0.4 - 0.9	0.193
0.1 - 0.4	0.0378

1.25, 1.25, 1.05, and 0.7. These relative power values are very close to the average value of Eq. 1 over the subregion. The cask total heat generation rate is 17.52 kW, or 59,783.5 Btu/hr. Dividing this by the source region volume of 247.55 ft³ (30.75 in. radius, 144 in. height) yields an average heat generation level of 241.5 Btu/ft³-hr. Multiplying this by the relative power factors above yields heat generation levels of 169.05, 253.58, and 301.88 Btu/ft³-hr. These values are used in the six axial subregions in the ANSYS thermal model.

The thermal analyses also model the effects of solar heating during transport. A horizontal cask with the sun directly overhead was considered. In this case, no solar heat is deposited on the cask ends. A typical insolation of 780 W/m² is assumed, and the overpack is assumed to be coated with white paint. Textbook data give an absorptivity of 0.26 for white paint, so the value 0.3 was used to account for some level of dirtiness. This yields an absorption rate of 234 W/m² on cask surfaces directly facing the sun. This is equal to 74.2 Btu/hr-ft².

The transportation overpack is 7.8333 feet wide, so its projected area is 7.8333 ft² per foot of cask length. Therefore, the solar heat generation is 581.2 Btu/hr per foot of cask length (74.2 x 7.8333). Since the thermal analyses are only two-dimensional at this phase of the design (azimuthally symmetric), this heat generation rate is spread out over the entire cylindrical surface of the overpack sidewall.

For simplicity, this heat generation rate is modeled as a volumetric heat generation in the overpack steel shell. Because the overpack is only 2-in. thick and has a high heat conductivity, no significant radial temperature gradient within the material is expected. Therefore, the surface heat flux can be modeled as an internal volumetric generation without affecting the analysis results.

The volume of the overpack (47 in. outer radius, 45 in. inner radius) is 4.014 ft³ per foot of cask length. Dividing the heat generation rate of 581.2 Btu/hr (per foot) by the overpack material volume of 4.014 ft³ (per foot) yields a volumetric heat generation rate of 145 Btu/ft³-hr within the overpack steel. This heat generation is applied over the entire length of the overpack.

2.2 Cask Model Geometry and Materials

The DUCRETE cask transportation system geometry and materials used in the thermal and shielding models are described in detail in this section. The manual structural calculations presented in Section 3 are also based upon the data presented here.

2.2.1 Model Geometry

The geometry and dimensions of the DUCRETE cask inside the transportation overpack are illustrated in Figure 3. The inner canister has an internal cavity that is 30.75 in. in radius and 180 in. long. In the shielding models, the bottom 4 in. of the cavity is filled with a homogenous mass that represents the fuel support sleeve steel and the assembly bottom end fittings. The next 144 in. are filled with a homogenous mass representing the fuel, the cladding, and the support sleeves. The remainder of the cavity is filled with another mass

representing support sleeves and assembly top hardware. All of these cylindrical homogenous regions have a radius of 30.75 in.

For the thermal analyses, the canister is filled with a single homogenous mass that extends the entire length of the fuel sleeve. The mass fills the whole cavity except for a 0.5 in. space of pure helium gas at the top of the cavity. This space is modeled because the assemblies and fuel sleeves stop just below the cavity top, leaving a gap of about 0.5 in., and the greatly reduced heat transfer across this region must be modeled.

The canister has a 0.75 in. thick outer shell, a 1 in. thick bottom plate, and a 12.5 in. thick top lid. Thus, the total canister height is 193.5 in. The inner cavity of the DUCRETE cask is assumed to have the same height as the canister (in the actual final design, the DUCRETE cask cavity may be slightly taller). The DUCRETE cask inner cavity has a radius of 33.5 in., leaving a 2 in. (radial) space around the canister. This gap represents the ventilation duct. The DUCRETE cask inlet and outlet duct work is to be designed at a later phase and is not modeled in the structural, thermal, or shielding analyses. VSC system experience shows that duct structures can be designed for concrete storage casks without creating unacceptable levels of radiation streaming. Also, the duct inlet and outlet will be at the cask corners, which will be an area of relatively low surface dose rates.

Two steel rings (shown in Figure 3) are welded to the DUCRETE cask inner cavity wall to suspend and secure the inner canister in the center of the DUCRETE cask cavity during transport (when the system is horizontal). They must do this without interfering with the ventilation duct during storage mode. Therefore, the upper ring is placed just above the top end of the canister's internal cavity, with the outlet duct right below it, and the bottom ring rests at the bottom of the DUCRETE cask's inner cavity, with the cask air inlet duct just above it. The air gap between the two steel rings (shown in Figure 3), which is the ventilation duct, covers almost all of the canister internal cavity and includes the entire active fuel region where the heat is being generated (the active fuel region begins 4 in. above the cavity bottom and ends 32 in. below the cavity top).

The rings have an outer radius of 33.5 in. (equal to the DUCRETE cask cavity radius) and an inner radius of 32 in. Thus, there is a 0.5 in. radial gap between the inner canister and the rings when the canister is lowered into the DUCRETE cask. (A 0.5 in. gap between canister and cask [storage or transport] is typical in current designs. The MPC specification³ calls for a gap of this size between the MPC and its transportation cask.) The bottom ring is 3 in. long, and the top ring is 4 in. long. The rings are about 180 in. apart.

The structural calculations presented in Section 3 show that the canister can handle the bending stresses caused by being suspended at its ends during drop events. These rings are not modeled in the thermal or shielding analyses (which is conservative).

The DUCRETE cask inner shell is 1.125 in. thick. The plate at the bottom of the DUCRETE cask inner cavity on which the inner canister rests is 1.5 in. thick. The DUCRETE cask outer shell is 0.5 in. thick, and the DUCRETE cask bottom plate is 1.25 in. thick. At the top end of the DUCRETE cask, a 1.75 in. flange joins the inner and outer shells. The thicknesses of the DUCRETE cask inner shell and bottom plates had to be

increased from the 0.5 in. thickness assumed in the initial storage mode analyses¹ to meet the stringent transportation structural requirements, as discussed in Section 3.

The DUCRETE shield is 9.375 in. thick along the cask wall. At the bottom end, the DUCRETE thickness is 6 in. The top of the DUCRETE cask is open (shielding is provided by the inner canister's steel top lid). There may be a heat transfer fin structure that passes through the DUCRETE and connects the inner and outer shells. These fins are not included in the geometrical models used in the shielding or thermal analyses. The thermal analyses model the presence of any fin structure by simply enhancing the thermal conductivity of the (homogenous) DUCRETE material.

The overall height of the DUCRETE cask is 202.25 in. It may actually be slightly longer if the internal cavity is made slightly longer than the canister, as mentioned above. The outer radius of the DUCRETE cask is 44.5 in.

In the transportation models, the DUCRETE cask sits inside the steel transportation overpack. A 0.5 in. gap is assumed to exist between the DUCRETE cask and the overpack on all sides. The overpack is a simple 2 in. thick steel cylinder with a 4.5 in. steel bottom plate and a 6 in. steel top lid. The thick end plates are required to meet transportation structural criteria. The top 6 in. of the overpack flare out an additional 1.5 in. to allow room for the bolts while maintaining a recessed closure design, which is a transportation requirement.

The overpack has an extensive array of heat transfer fins on its outer surface over the entire 144 in. heat generation region of the cask. The fins do not cover the entire cask length because of the impact limiters. The fins are annular, extending radially from the overpack. Thus, air may rise between the fins when the cask is in a horizontal orientation. The fin structure has not been formally designed, but the overpack surface heat transfer enhancement assumed in the thermal analyses can be achieved with aluminum fins 2 in. long and 1/8 in. thick, spaced 0.5 in. apart. If aluminum fins are used, the overpack will be clad (plated) with an aluminum coating about 1/8 in. thick. The fins are not directly modeled in the shielding or thermal analyses. The thermal analyses model the presence of the fins by using an enhanced surface convective heat transfer coefficient over the fin-covered area. The shielding analyses conservatively ignore the presence of the fins.

Impact limiters are modeled at the cask ends. The impact limiters will cover some portion of the cask sidewall as well, but this added too much complexity to the shielding and thermal models. Typical aluminum honeycomb transport cask limiters are about 24 in. thick on the ends. Therefore, the thermal analyses model 24 in. thick cylindrical regions at each cask end to represent the impact limiters. These regions extend out to the cask outer radius. The shielding analyses conservatively neglect the impact limiters.

Both the shielding and thermal analyses assume that the transportation overpack is surrounded by an infinite mass of ambient air. The shielding analyses calculate gamma and neutron fluxes across surfaces at various distances and directions from the overpack to verify compliance with various dose rate limitations for various locations.

The radial geometry of the DUCRETE cask transportation system along most of its length is summarized below. This information is also shown in Figure 3.

Radial Span (in.)	Cask System Component
0 - 30.75	Canister Interior Region
30.75-31.5	Canister Sidewall
31.5-33.5	Ventilation Duct
33.5-34.625	DUCRETE Cask Inner Liner
34.625-44.0	DUCRETE Shield
44.0-44.5	DUCRETE Cask Outer Shell
44.5-45.0	DUCRETE Cask/Overpack Gap
45.0-47.0	Transportation Overpack Shell

2.2.2 Cask Model Materials and Densities

Table 3 lists the materials used in each region of the DUCRETE cask system models. For each material type, the thermal conductivity and density are shown. The thermal conductivity data are used in the thermal analyses, while the density data are used in the cask weight and structural calculations.

The thermal conductivity and density of carbon steel were taken from the VSC system SAR.² The Type 304L stainless steel and aluminum alloy conductivities and densities are taken from an engineering text;⁵ the XM-19 values are assumed to equal that of 304L. The DUCRETE conductivity is taken from theoretical calculations performed by INEL,^a while the density was taken from Reference 1. Many of the cases studied assume a heat transfer fin structure through the DUCRETE material. The fin structure is modeled in the thermal calculations by using a higher DUCRETE thermal conductivity. The calculation of the effective DUCRETE region conductivity is discussed in Section 4.

Both the thermal and shielding analyses model the complicated geometry inside the inner canister with simple homogenous masses of material because the internal geometry is too complicated to model explicitly. Fortunately, details of the canister interior geometry do not significantly affect dose rates, so accurate results can be obtained with the material inside the canister "smeared" into a homogenous mixture.

The homogenous material inside the inner canister has separate axial and radial conductivities. The axial conductivity is primarily due to conduction through the fuel support sleeve structure and the zircaloy fuel cladding; heat conduction through the fuel itself is conservatively neglected. Thus, axial conductivity is based upon the MPC canister internal structure. In Sierra Nuclear's proposed MPC design, the fuel support sleeves consist of

a. Personal communication, R. J. Kochan to W. J. Quapp, "Effective Thermal Conductivity of Concrete with UO₂ Aggregate--Preliminary Estimate," February 1, 1994.

Table 3. DUCRETE Cask Model Materials.

Cask Model Region	Material Type	Thermal Conductivity (Btu/hr-ft-°F)	Density (lb/in ³)
Canister interior cavity	Homogenized mixture	Axial = 4.8 Radial = 2.0	0.104
Canister shell, bottom plate, and top lid	304L stainless steel	8.6	0.286
DUCRETE cask inner and outer shells and bottom plates	SA 516 carbon steel	26.0	0.284
DUCRETE shield	"DUCRETE"	1.16 ^a	0.1852
Transportation overpack shell, bottom plate, and top lid	XM-19 stainless steel	8.6	0.286
Impact limiter	Aluminum honeycomb	Axial = 5.0 Radial = 1.5	~ 0.015
Void regions and gaps	Helium (or air)	0.127 (0.016)	0

a. Higher effective DUCRETE conductivities are often used to account for the presence of heat transfer fins. A case that assumes the standard concrete conductivity (0.72 Btu/hr-ft-°F) is also studied.

9.625 in. (outer width) square tubes whose wall consists of a sandwich of 0.25 in. of stainless steel, 0.125 in. of aluminum, and a thin outer coating of 0.0625 in. of stainless steel. The axial heat conductivity is calculated by dividing the conductivity of each type of metal by the area fraction it occupies inside the canister (aluminum and zircaloy have conductivities of roughly 92 and 13 Btu/hr-ft, respectively). The entire area covered by each metal type (overall 24 fuel support sleeves) is divided by the inner cavity area (radius = 30.75 in.) to determine the area fractions. Although the axial conductivity of the VSC system canister is somewhat lower than that expected for the MPC canister, the VSC canister heat load will be lower, and the maximum allowed clad temperature is much higher, as discussed in Section 4. The MPC canister is modeled in the thermal analyses because it is the limiting case.

The radial conductivity assumed for the canister cavity region is actually not important because it only affects the maximum cladding temperature—it has no effect on the temperature distribution anywhere outside the internal canister. As discussed in Section 2.3, the peak cladding temperature is actually calculated from the maximum canister wall temperature calculated by the thermal analyses. The difference between the maximum clad temperature and the canister wall temperature is based upon thermal calculation results presented in the VSC system SAR.² A rough estimate of an effective radial conductivity, based on those same VSC analyses, was used in the thermal analyses.

The impact limiter region also has asymmetric conductivity. The axial value is calculated by multiplying the conductivity of the aluminum alloy by an estimate of the aluminum area fraction in the honeycomb structure. The "grain" of the honeycomb material runs in the axial direction. Due to the grain effect, the radial conductivity is significantly lower.

The canister interior density is calculated by taking the estimated total weight of the canister internals and dividing by the cavity volume. Fuel assembly weight was taken from the MPC specification. Fuel support sleeve weight was estimated from the dimensional information mentioned earlier. Transport analyses assume no water is present inside the canister. Impact limiter density is not used in either the shielding or thermal calculations. The impact limiter weight does not apply towards the 125 ton weight limit of the system. However, certain structural calculations presented in Section 3 are based upon the total system weight, including impact limiters. For these calculations, an impact limiter weight of 7000 lbs. is assumed. With respect to structural and weight calculations, the MPC canister densities are used because they are greater than those of the VSC system canister.

The elemental compositions used for each material type in the shielding models are described in Table 4. The average elemental densities for the canister interior regions were taken from the standard VSC system SAR. Use of the VSC canister densities in the shielding analyses is conservative because the MPC system canister is expected to have a higher overall average internal density. Using the higher MPC canister radiation source along with the VSC system canister's internal average densities is a maximally conservative approach.

The DUCRETE material description in Tables 3 and 4 is for DUCRETE that employs colemanite sand as a fine aggregate and has UO_2 rock occupying 45% of the volume within the DUCRETE material. The colemanite sand occupies 2/3 of the remaining volume (36.7% of the total) and cement occupies the rest (18.3%). As the studies presented in Reference 1 show, the optimum DUCRETE composition depends upon the radiation source term used in the analysis. The above composition is a compromise composition that produces dose rates near the optimum for all of the spent fuel sources studied in Reference 1 (the reference gives detailed information on DUCRETE composition and how it is calculated).

2.3 Analytical Methodology

2.3.1 Shielding Analysis

The shielding analyses were performed with the MCNP monte-carlo shielding code. The code allows explicit three-dimensional models of a system with explicit material descriptions of each geometrical region. The code handles neutron and gamma transport and treats all significant forms of interaction between the gammas and neutrons and the cask materials. Homogenous gamma and neutron sources are placed in the canister interior region. The source spectra shown in Tables 1 and 2 can be directly entered into the code.

The code outputs the neutron and gamma surface fluxes within an energy bin structure specified by the user. The flux in each energy bin is multiplied by a flux-to-dose conversion factor for that energy level. This factor, which is a function of particle energy level, has units

Table 4. Material Composition of DUCRETE Cask Model Regions Used in Shielding Analyses.

Cask Model Material	Component Elements	Elemental Densities (g/cm ³)
Canister Interior (homogenized mixture)	uranium	2.123
	oxygen	0.222
	zirconium	0.385
	<u>iron</u>	<u>0.473</u>
	total	3.203
Carbon Steel	iron	7.870
Stainless Steel (304L & XM-19)	chromium	1.5049
	manganese	0.1584
	iron	5.5050
	<u>nickel</u>	<u>0.7525</u>
	total	7.9208
Air (He modeled as air)	nitrogen	9.76e-4
	oxygen	3.00e-4
	<u>argon</u>	<u>1.67e-5</u>
	total	1.29e-3
DUCRETE	uranium	3.1741
	hydrogen	3.11e-2
	boron	0.1374
	oxygen	1.2562
	magnesium	8.89e-3
	aluminum	2.15e-2
	silicon	6.02e-2
	sulfur	4.01e-3
	calcium	0.4332
	<u>iron</u>	<u>1.21e-2</u>
	total	5.1385

of mrem/hr per particle/cm²-sec. The neutron and gamma flux-to-dose conversion factors are shown in Tables 5 and 6, respectively.

Over a specified surface at a given location, the code outputs the particle flux per source particle generated. These values are multiplied by the particle generation rates to yield actual surface fluxes. These fluxes are, in turn, multiplied by the flux-to-dose conversion factors to yield dose rates on the surface. The total particle generation rates for the MCNP models are found by multiplying the per assembly gamma and neutron source rates listed in the MPC specification³ by the cask payload of 24 assemblies.

Four MCNP models of the DUCRETE transportation cask system were developed. A finite height cylindrical model, shown in Figure 4, was developed to predict the peak gamma dose rate on the side of the transportation overpack and 2 m from the overpack surface.

Table 5. Neutron Flux-to-Dose Conversion Factors.

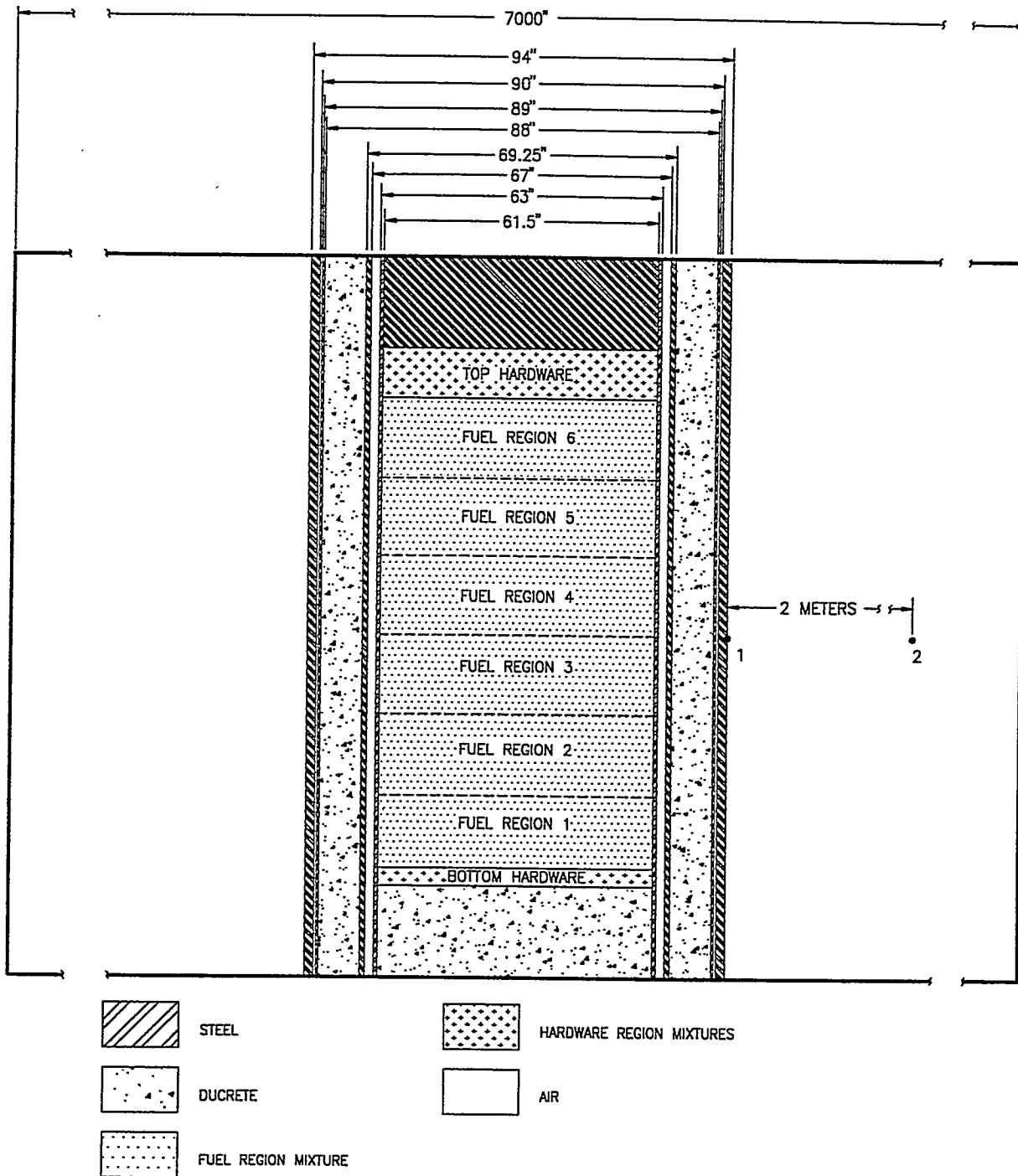
"CASK" and ANISN-PC Group Number	Group Upper Bound Energy (MeV)	Flux-to-Dose Conversion Factor (millirem/hr <i>per</i> neutron/sec-cm ²)
1	14.92	0.2088
2	12.2	0.1656
3	10.0	0.1476
4	8.18	0.1476
5	6.36	0.1404
6	4.96	0.1332
7	4.06	0.1296
8	3.01	0.1260
9	2.46	0.1260
10	2.35	0.1296
11	1.83	0.1332
12	0.55	0.1188
13	0.111	0.0540
14	3.35e-3	0.00648
15	5.83e-4	0.00432
16	1.01e-4	0.00468
17	2.90e-5	0.00468
18	1.01e-5	0.00450
19	3.06e-6	0.00432
20	1.12e-6	0.00414
21	4.14e-7	0.00396
22	1.00e-8	0.00378

Table 6. Gamma Flux-to-Dose Conversion Factors.

"CASK" and ANISN-PC Group Number	Group Upper Bound Energy (MeV)	Flux-to-Dose Conversion Factor (millirem/hr per neutron/sec-cm ²)
1	10.0	9.792e-3
2	8.0	8.280e-3
3	6.5	6.840e-3
4	5.0	5.760e-3
5	4.0	4.752e-3
6	3.0	3.960e-3
7	2.5	3.492e-3
8	2.0	2.988e-3
9	1.66	2.412e-3
10	1.33	1.908e-3
11	1.0	1.602e-3
12	0.8	1.260e-3
13	0.6	9.216e-4
14	0.4	6.372e-4
15	0.3	4.392e-4
16	0.2	2.376e-4
17	0.1	1.404e-4
18	0.05	3.024e-4

(These locations were chosen because regulatory dose rate limits apply to them.) This case models the axial gamma source distribution in the fuel, as described in Section 2.1.1. The source region is divided into six axial subsections that have different gamma source densities. For each of the analyzed surfaces (the cask surface and 2 m from the cask), dose rates are calculated over a narrow axial span that lies directly over the section of the cask with the highest gamma source strength. This case does not accurately model the cask ends as they are not used to study cask end dose rates. Large masses of steel and DUCRETE are placed at the ends of the model, however, to roughly model any scattering in the cask ends that may redirect particles back towards the cask side. The model is two-dimensional and azimuthally symmetric.

Two finite slab models were developed to calculate gamma dose rates on the transportation overpack bottom end. They accurately model the materials and thicknesses of the bottom shielding. Radially, the models extend outside the radius of the source region. One model calculates the dose rate contribution from the bottom end fitting source (as described in Section 2.2.1). The other calculates the contribution from the fuel region gamma source. The geometry and materials are identical for the two models, see Figure 5; the only



03-2015-0243 C:\ACOMB\AC003\HARSH\SK125

Figure 4. Finite height cylinder (R-Z) MCNP gamma model of the DUCRETE cask transportation system. Peak gamma dose rates were calculated for the overpack side surface (1) and 2 m from the cask side (2).

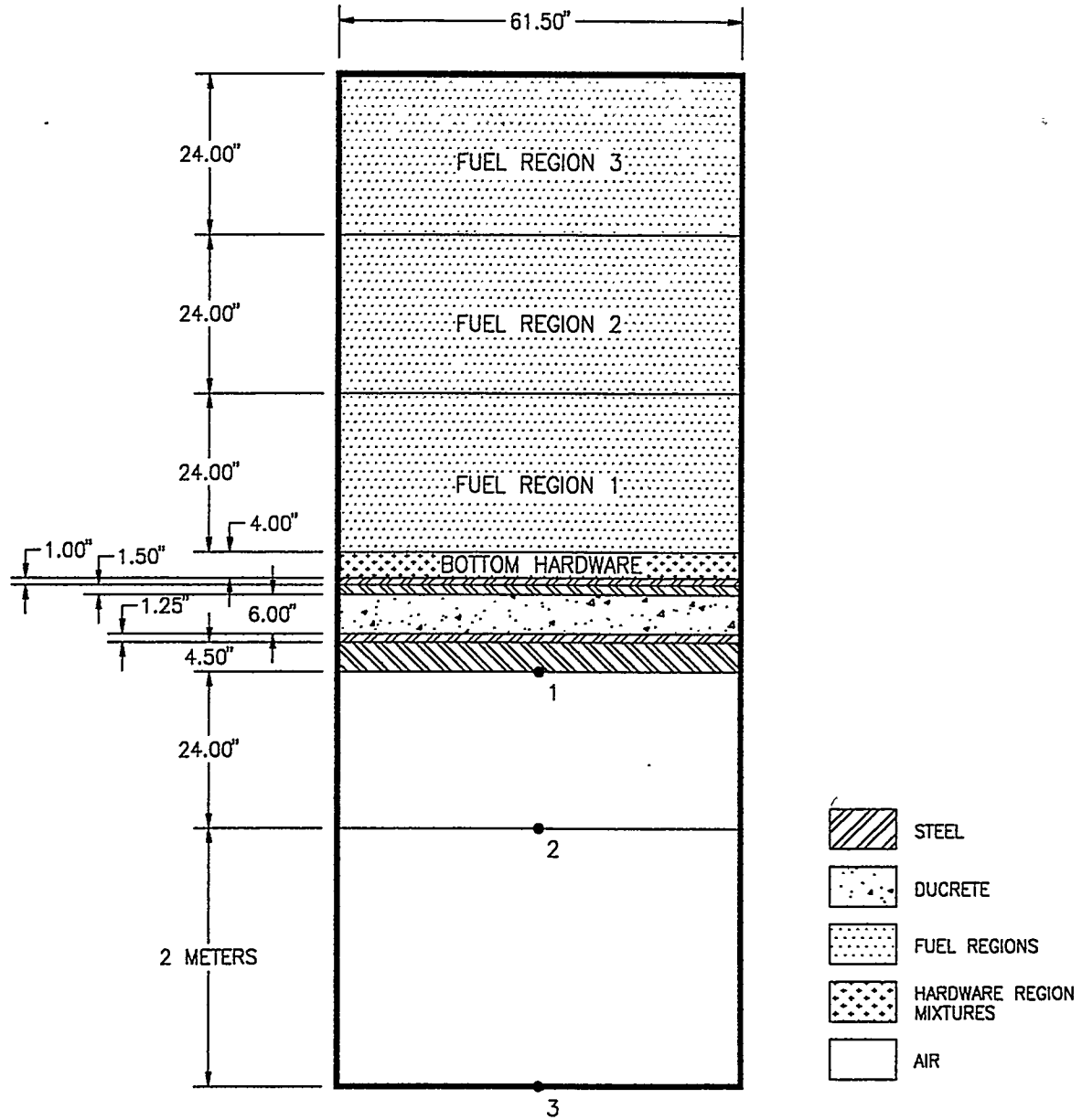


Figure 5. Slab (1-D) MCNP model of the DUCRETE cask bottom end. Fuel region and bottom hardware source runs were performed. Gamma dose rates were calculated at the overpack bottom surface (1), the bottom impact limiter, bottom surface (2), and 2 m from the bottom impact limiter (3).

differences between the two models are the characteristics and locations of the gamma sources. As discussed in Section 2.2, the fuel region model only extends halfway through the fuel source region, since the fuel in the top half of the cask does not contribute significantly to cask bottom end dose rates. This model accounts for the axial source distribution in the fuel by dividing the bottom half of the fuel region into three axial subsections with different gamma source densities. Note that the MCNP output fluxes for this model are only multiplied by half of the total cask source rate since only half of the fuel source region is modeled.

These two models calculate dose rates on the DUCRETE storage cask bottom, the transportation overpack bottom, the impact limiter bottom, and 2 m from the impact limiter bottom. Regulatory limits only apply to the last two locations, but the dose rates at the other locations are of interest for minimizing radiation exposure.

Finally, a full two-dimensional (R-Z) model of the entire cask (shown in Figure 6) was developed to calculate neutron dose rates. This two-dimensional model accurately describes the cask sides as well as the cask system top and bottom ends. Peak dose rates (over the "hottest" fuel region) are calculated on the cask side surface and 2 m from the cask side. Dose rates are also calculated at the overpack bottom surface, at the bottom impact limiter surface, 2 m from the bottom impact limiter, and on the overpack top end surface. Dose rates on the top impact limiter surface and 2 m from the top impact limiter are estimated using the bottom end results and the ratio between the top and bottom surface dose rates. For neutrons, MCNP can model the entire cask geometry and obtain dose rates at all of these locations in the same run. For gammas, this approach causes the run time to be too long, so the cask side study and the cask end study had performed separately.

Neutron dose rates were not determined at the DUCRETE cask bottom surface because they are known to be a very small fraction of the dose rate at that location. They are also known to be smaller than those calculated for the bottom of the standard VSC system transfer cask. This is discussed further in Section 5. Also, gamma dose rates on the cask top end were not analyzed because they are known to be extremely small, as discussed in Section 5.

An infinite cylindrical MCNP analysis of the DUCRETE storage cask, like the original analyses,¹ was performed using the dimensions and materials described in this report because some minor changes in the storage cask design were required to meet the transportation structural criteria. The purpose of the re-analysis was to assess any effect these changes had on the peak surface dose rates for the storage cask. This MCNP model is shown in Figure 7.

For each of the MCNP models shown in Figures 4 through 7, the model cuts off where the heavy black line is shown. Particles reaching this surface are eliminated. However, the MCNP models all include a huge volume of air around the cask geometry to capture any particle scattering (or "skyshine") effects.

For a given cask and overpack, if the storage cask surface dose rate and the transportation overpack dose rate are known, the dose rate ratios can be established. With these ratios, it is possible to develop a formula for storage cask surface dose rates limits for transportation. Storage casks with higher surface dose rates will be known to produce unacceptable dose rates on the overpack surface or 2 m from the overpack surface.

For reasons discussed in Reference 1, a correction factor of 1/3 was applied to MCNP dose rate predictions for the DUCRETE storage cask surface. The correction factor is based upon extensive comparisons between MCNP predicted dose rates and measured dose rates for VSC storage cask systems [both the concrete storage cask and the (steel and lead) transfer cask]. The same correction factor is applied to cask side results in the analyses performed for this report. No correction factor is applied to cask end results.

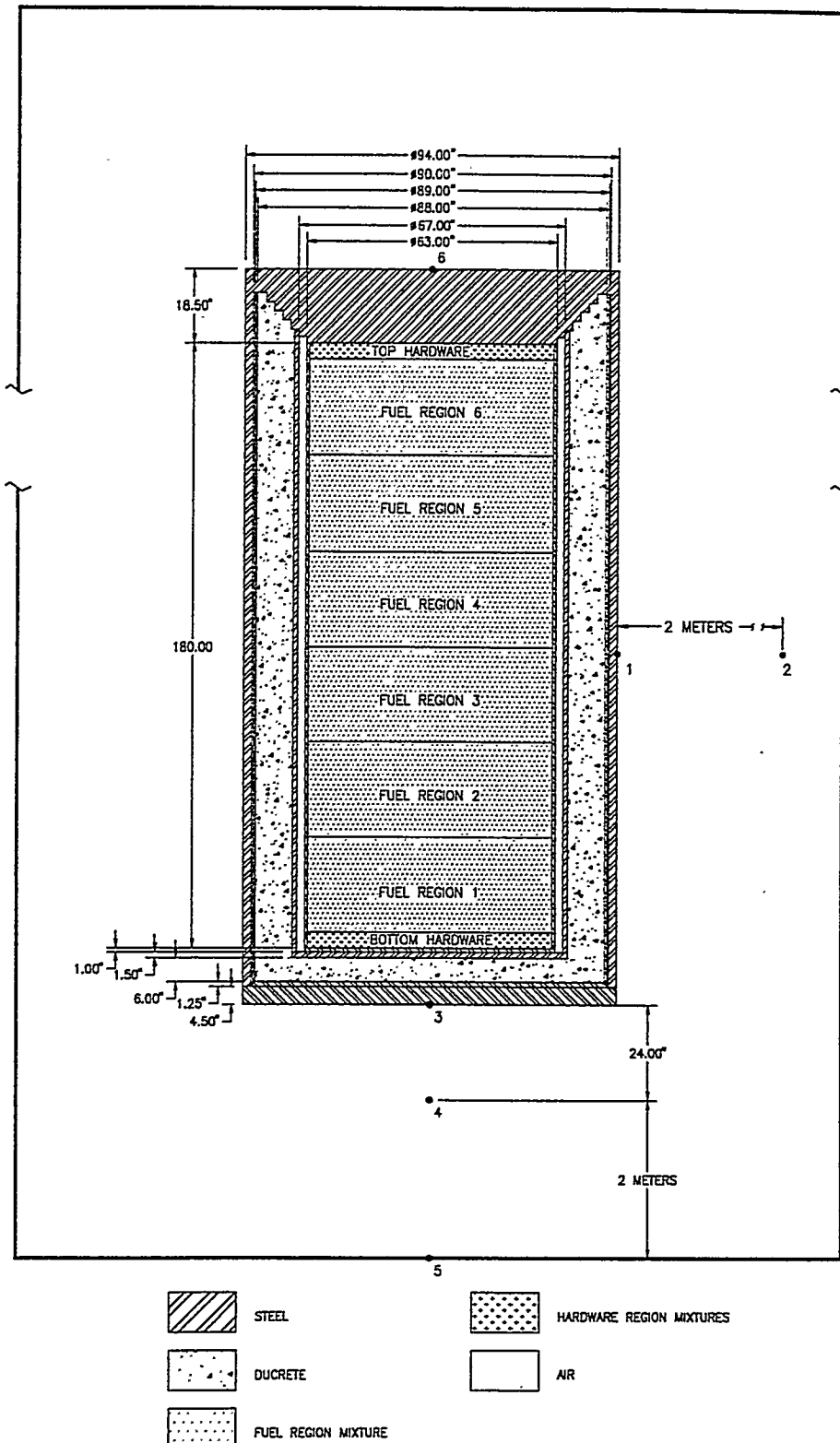


Figure 6. Two-dimensional (R-Z) MCNP neutron model of the DUCRETE cask transportation system. Peak neutron dose rates were calculated for the overpack side surface (1), 2 m from the overpack side (2), the overpack bottom surface (3), the bottom impact limiter bottom surface (4), 2 m from the bottom impact limiter (5), and the overpack top surface.

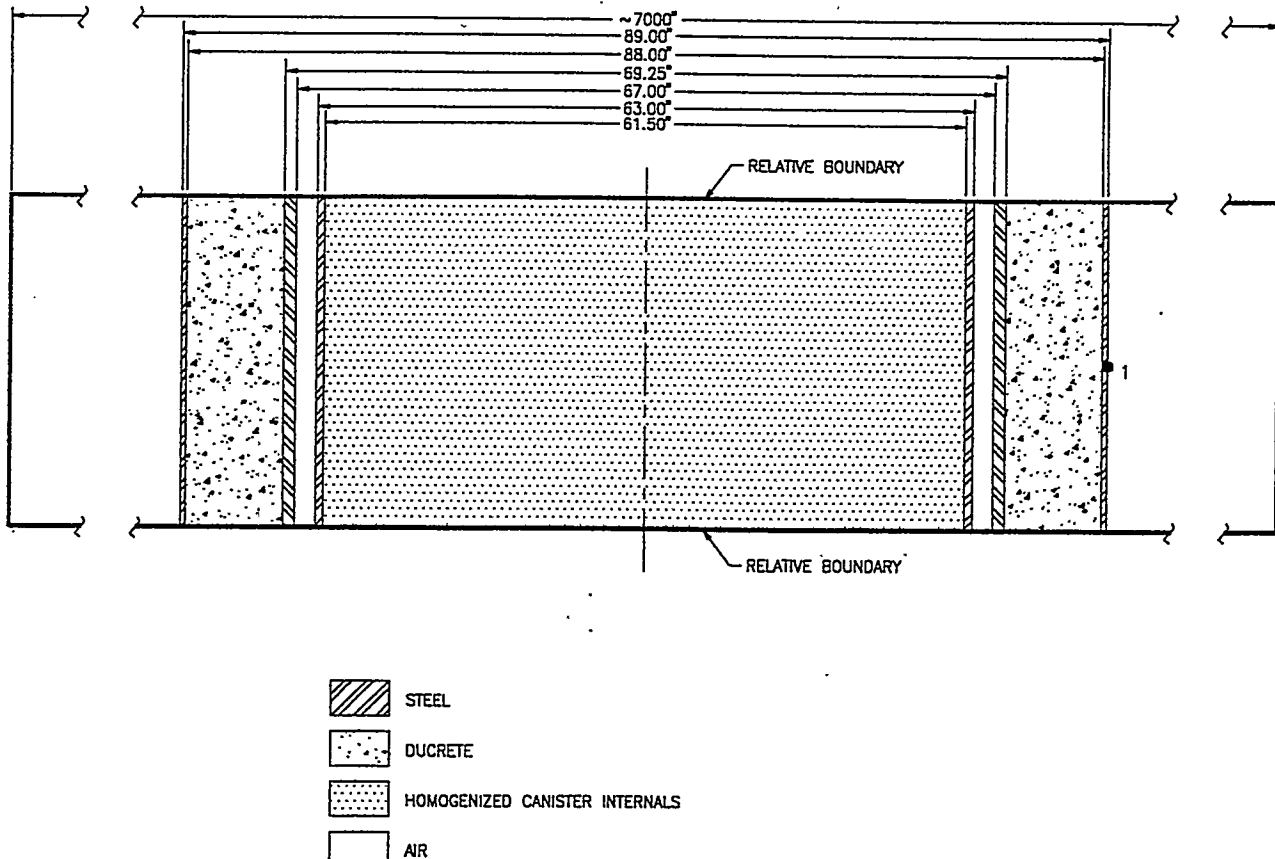


Figure 7. Infinite cylindrical (1-D) MCNP models (gamma and neutron) of the DUCRETE cask. Peak dose rates on the cask surface were calculated.

2.3.2 Thermal Analyses

DUCRETE cask system temperatures during transport are calculated using the ANSYS finite difference code, an industry standard code that is commonly used in spent fuel cask thermal analyses. A two-dimensional (azimuthally symmetric) ANSYS model of the DUCRETE storage cask inside the transportation overpack was developed using the geometry and material data presented in Section 2.2. A vertical cross section of this model is illustrated in Figure 8, which shows all of the nodes (dots) of the model and the rectangular elements whose boundaries are defined by the nodes. The material occupying each model region is also illustrated. The arrows in Figure 8 represent radiative heat transfer links between nodes on opposite sides of gaps in the geometry (or between nodes on the overpack exterior and the ambient environment).

In actuality, the ANSYS model describes a narrow wedge (7.5 degrees) of the cask. Adiabatic boundary conditions are applied at the wedge boundaries (except at the outer edge) to model the entire (azimuthally symmetric) geometry. A large 2-D array of node points is defined on the 0° vertical plane (the cross section shown in Figure 8). Node points are required at all material boundaries. Additional node points may be placed within material regions as well. A similar 2-D matrix of node points is defined along the 7.5° plane. The

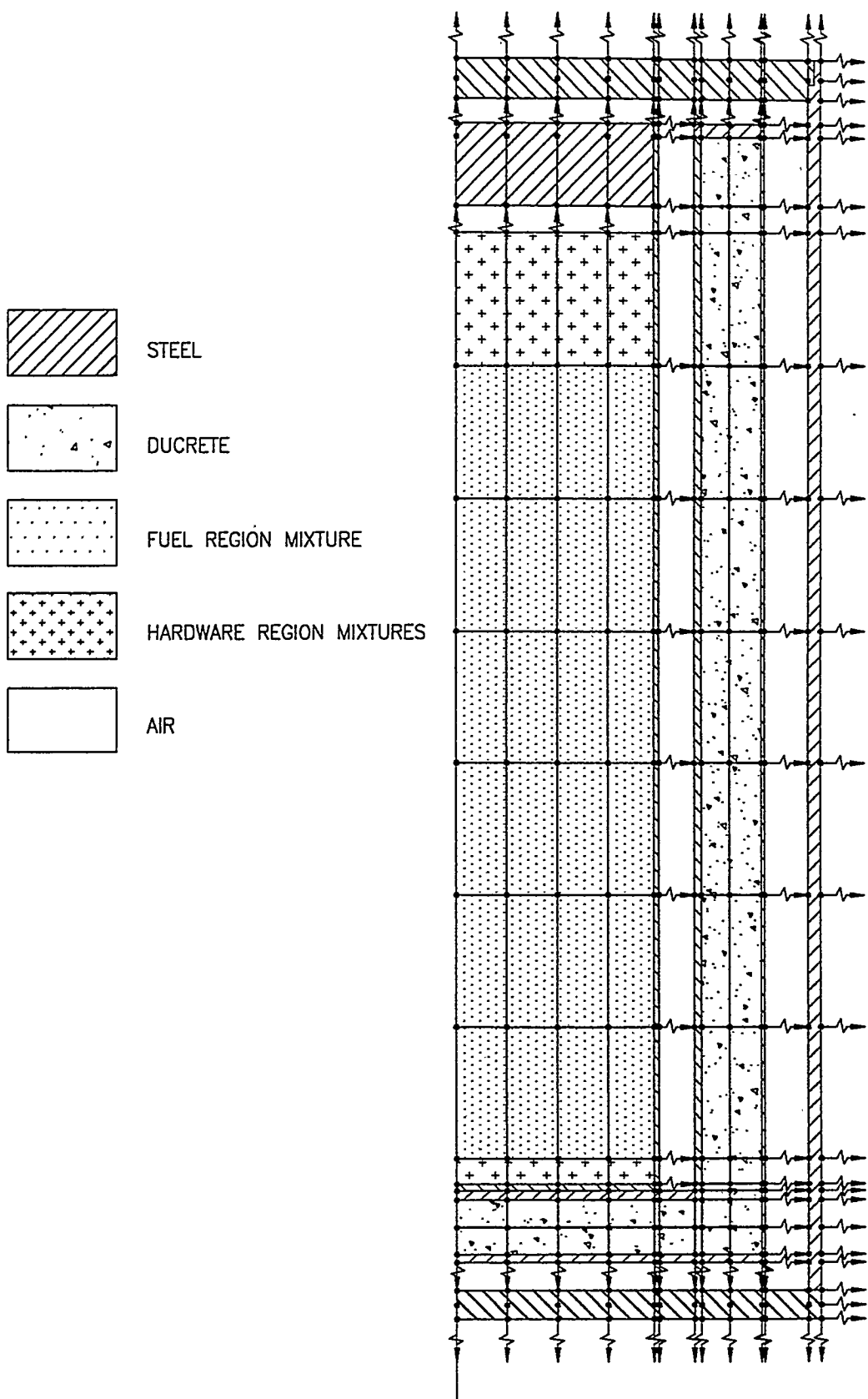


Figure 8. ANSYS finite difference model of the DUCRETE cask transportation system (vertical cross section view). Arrows indicate radiation links between nodes. The size of system gaps is increased in this figure to show radiation links.

two matrices of node points along the two planes define the three-dimensional wedge model. The model is defined using polar coordinates.

Sets of eight node points define the eight corners of rectangloid regions, or "elements". These elements are filled with material types and their corresponding properties. Each element has a specified conductivity, density, and heat capacity (although the density and heat capacity do not affect steady-state thermal analysis results). The element may also have a defined volumetric heat generation rate. The code-calculated heat conduction rates between adjacent nodes are based upon the material conductivity and the temperature difference between the nodes.

The complete set of node locations, the elements they define, and the materials specified for each element explicitly define the azimuthally symmetric cask system geometry shown in Figure 3. In the ANSYS model, the fuel assemblies and fuel assembly support structure inside the inner canister are modeled as a homogenous mass of material. This material fills the canister interior except for a 0.5 in. gap of pure helium at the top of the cavity. This material has a separate axial and radial thermal conductivity, as discussed in Section 2.2.

The ANSYS code also treats heat transfer from natural convection and radiation. A surface convection coefficient is defined for groups of nodes on the cask surface. The code then applies that coefficient to all rectangular surfaces bounded by those nodes. The convective heat transfer from a specified group of nodes is equal to the surface area times the convection coefficient times the temperature difference between the nodes and the ambient air temperature, which is a single constant value specified by the user. For the thermal analyses, the ambient air temperature is set at 100°F—transportation regulations require this temperature to be assumed as a worst case condition.

The surface convection coefficients used for the overpack outer surface are based upon conservative natural convection formulas taken from engineering texts.⁵ The convection coefficient for the side of a horizontal cylinder with the overpack's dimensions is 0.75 Btu-hr-ft-°F. The vertical plate formula was used to determine the coefficient for the overpack ends (actually the impact limiter ends). In using this formula, the disk-shaped cask end was treated as a square of equal area. This convection coefficient is calculated to be 0.65 Btu/hr-ft-°F. As mentioned earlier, the section of the overpack outer surface that lies over the active fuel region inside the canister is covered with an extensive array of aluminum fins. The fin structure is not directly modeled in the ANSYS analyses—it is modeled by using an enhanced surface convection coefficient for that section of the overpack side. A surface convection coefficient of 2.5 Btu/hr-ft-°F is assumed for this section of the overpack (a coefficient of 0.75 is assumed for the rest). The fin structure is described in Section 4.1.1.

For all gap and void regions inside the cask system, convection effects are conservatively ignored in the thermal analyses.

Radiation is treated in a fashion similar to convection. For each node that borders the outside air or any void or gap in the model, the user inputs the following information: the emissivity of the surface the node is on, the view factor between the surfaces, and the surface

area covered by the node point (the boundaries of the node point "areas" are defined as being the midpoints between the nodes). A node point on the other side of the void that the heat will be going to must also be specified. For model gap regions, these nodes are simply the nodes on the other side of the gap. For the cask outer surface, nodes are defined at arbitrary points in space that "receive" the radiation leaving the cask surface nodes. Based on the node areas, the surface emissivity, and the temperature difference between the node pairs, the ANSYS code calculates radiative heat transfer rates from the specified groups of nodes.

The code uses the standard radiation formula to determine radiative heat transfer between the nodes:

$$H = A * \epsilon * F_v * \sigma (T_1^4 - T_2^4)$$

where A is the node area, ϵ is the surface emissivity, F_v is the view factor between the surfaces, σ is the Stephan-Boltzman constant, and T_1 and T_2 are the temperatures of the two node points.

An emissivity of 0.8 is assumed for the internal gaps in the cask system. This is a typical value for rough unpolished metal surfaces and is used in the VSC system SAR.² The overpack outside surface, which is assumed to be coated with white paint, has an emissivity of 0.9. Engineering texts⁵ give emissivities greater than 0.9 for white paint, and surface dirt or dust will not reduce the emissivity. A view factor of 1.0 is assumed for all of the surfaces because all radiation leaving an inner cylindrical shell will hit the outer shell surrounding it. Radiation exchange with the outside air also has a view factor of 1.0. The node temperatures are calculated by the ANSYS code as part of a converged steady-state solution. The temperature of the distant ambient air node points (used for radiation exchange between the cask outer surface and the ambient environment) is specified (constrained) at the temperature of the ambient air.

Using the data input by the user, the ANSYS code determines the heat transfer between nodes as a function of the temperatures of the nodes. The calculated heat transfer accounts for conduction, radiation, and convection. The code iterates until a converged set of node temperatures is found that yields consistent heat transfer rates between the nodes and removes all of the heat generated within the system.

As mentioned in Section 2.2, the ANSYS model is not used directly to calculate peak fuel cladding temperatures. The ANSYS model is used to determine temperatures at locations outside the inner canister and the peak canister shell temperature. The difference between the canister shell temperature and the peak clad temperature is taken from another analysis. In the ANSYS model, the structure inside the canister is mixed into a simple homogenous material. The axial and radial conductivities of that material are calculated as discussed in Section 2.2.2. The radial conductivity is not important to the ANSYS calculations since it does not affect any temperatures outside the canister. The axial conductivity of the canister internals has some effect on temperatures outside the canister, since a lower axial conductivity would lead to a greater amount of peaking in the canister wall temperature. Fortunately, the calculation of the axial conductivity of the canister internals is straightforward (as discussed in Section 2.2.2). A rough estimate of the radial conductivity is used in the ANSYS models.

A detailed infinite height ANSYS model of the VSC system canister's internal geometry was developed and presented in the VSC system SAR.² The fuel sleeve array geometry was explicitly modeled. The fuel assemblies were modeled as rectangular regions with an effective axial and horizontal conductivity. This model considers conduction through the support sleeves, radiation between the assemblies and the sleeves, radiation between the sleeve array and the canister wall, and convection in some large helium-filled regions between the basket outer edge and the canister shell. The effective axial conductivity for the fuel assembly region is easily calculated. An effective horizontal (radial) heat conductivity for the assemblies was calculated based on experimental measurements on fuel assemblies.² This effective conductivity covers all of the complicated radiative and convective heat transfer occurring between the fuel rods. In this model, the canister wall temperature is input by the user. The model then determines the temperature distribution throughout the basket structure, including the peak cladding temperature. Basically, the model determines the temperature difference between the peak canister wall temperature and the peak fuel clad temperature.

To model an MPC canister in a horizontal orientation, the above model was re-run with some minor modifications. The conductivity of the fuel sleeve steel was doubled. This reflects the fact that the 1/8 in. aluminum plates that will be used in the MPC canister have double the overall heat conductivity of the 3/16 in. carbon steel sleeve walls in the VSC system canister. Due to the horizontal canister orientation, little convection is expected in any of the canister void regions. Therefore, convection is not included in the canister interior helium regions. The conductivity of helium is ~ 0.11 Btu/hr-ft $^{\circ}$ F. However, a conductivity of 0.5 is used for the space between the sleeves and the canister wall because aluminum heat transfer members that will extend across this region in the MPC canister.

Another version of this model was developed for the horizontal VSC system canister. In this model, the fuel sleeve conductivity is not doubled. The only change from the original model is to eliminate convection from the large helium voids in the canister. A helium conductivity of 0.11 Btu/hr-ft $^{\circ}$ F is assumed.

The heat load for the MPC canister version of the model was set at 17.52 kW. For the VSC system canister, the heat load was set at 16 kW. A peak cask shell temperature of 400 $^{\circ}$ F was used for the MPC model, and a canister wall temperature of 375 $^{\circ}$ F was used for the VSC canister model. These models determine the difference between the peak clad temperature and the peak shell temperature. This result will vary little with the canister temperature, the only slight variation being due to radiation effects. The selected shell temperatures are based on initial estimates of the actual calculated shell temperatures.

The final result of these canister internal models is the difference between peak clad and peak shell temperatures for the MPC canister and for the VSC system canister. The ANSYS thermal analyses on the DUCRETE cask system presented in this report are used to determine peak canister wall temperatures for each studied case. Then the temperature differences are added to these peak shell temperatures to determine the peak clad temperatures. The rough estimate of canister radial conductivity used in the ANSYS analyses is based upon the temperature differences ($T_{clad} - T_{shell}$) calculated by the basket internal analyses.

2.3.3 Structural Analyses

The structural adequacy of the DUCRETE cask system in transportation mode was verified using manual calculations based upon conservative formulas. Formulas for calculating stresses and required material thicknesses were taken from engineering texts and from the Oak Ridge Cask Designer's Guide.⁶ This reference gives formulas that specifically apply to spent fuel casks and the loads associated with the regulatory requirements for transportation casks. The formulas give stresses and required material thicknesses as fairly simple functions of cask parameters.

The steel transport overpack provides primary structural support for the system and is responsible for meeting all of the transportation regulatory structural criteria. The DUCRETE cask is not a containment boundary. It is only required to support its own weight and prevent the DUCRETE material from crushing the canister during drop events. Transport regulations require events such as a 30 ft drop onto an unyielding surface (from any angle), a 6 in. drop onto a narrow post, and the immolation of the cask to be analyzed. None of these events may breach the containment boundary. In Section 3, each event that requires analysis is listed along with manual calculations that verify the adequacy of the proposed cask system.

The analyses assume maximum possible component weights. The canister weight is assumed to be 37.5 tons (dry weight, since the canister is drained of water before transport). Subtracting the weight of the canister lids and shell (9.8 tons) leaves 27.7 tons in the canister interior. This load is assumed to be evenly distributed (like a fluid), resulting in a load of ~310 pounds per in. of canister length. For DUCRETE cask calculations, the material densities shown in Table 3 are assumed.

For calculations of the overpack's ability to withstand drop and puncture events, the entire loaded overpack weight is assumed to be 132 tons. This weight is based upon the maximum allowed transportation overpack weight of 125 tons plus an estimated 7 tons for the impact limiters (assuming impact limiters with an outer diameter of ~130 in. and an overall length of 36 in., 24 of which extend past the cask end). The average density of the impact limiter volume is ~30 lb/ft³. These dimensions and densities are typical for rail cask impact limiters. The impact limiter weight does not apply towards the 125 ton transportation cask weight limit since they are not lifted with the cask; they are placed on the cask after it is placed on the rail car. The impact limiter weight is present, however, during the hypothetical accident events.

3.0 STRUCTURAL EVALUATION

The structural adequacy of the transportable DUCRETE cask system is verified using manual calculations and conservative formulas from engineering texts. The formulas give upper bound estimates of material stress levels. More refined analyses, such as computational finite element analyses, will yield lower stress levels. Such analyses would be performed in a DUCRETE cask formal design effort.

The transportation overpack is assumed to have impact limiters on its ends that limit the system peak acceleration to 44 g's in a 30 foot horizontal drop event and to 124 g's in vertical drop events (i.e. the cask being dropped on its top or bottom end). These performance parameters are typical of impact limiters that have been used with rail casks in the past. To achieve this performance, impact limiter dimensions and weights such as those mentioned in Section 2.3 will be required.

Based on the acceleration levels given above, the DUCRETE cask system must be shown to meet all of the transportation structural criteria. In general, the DUCRETE transportation system is expected to be structurally adequate since it is in many ways comparable to typical, licensed spent fuel rail transportation casks. Such casks typically have a 1.125 to 1.25 in. inner shell, about 4 in. of lead shielding, and a ~2.5 in. stainless steel main structural shell. In the DUCRETE cask system, the DUCRETE cask inner shell is comparable to the transportation cask inner shell, the DUCRETE material is comparable to the lead, and the overpack shell is comparable to the main structural shell. In both cases, the inner shell must be thick enough to take the slumping loads of the shielding material, which is assumed to have no structural strength.

The DUCRETE cask inner shell is 1.125 in. thick, comparable to typical rail casks. Both systems have a "fluid-like" shielding material shell. The DUCRETE and the lead in transportation casks are of similar total mass. Finally, since it is made of a stronger than usual stainless steel type (XM-19), the DUCRETE cask system's overpack shell is as strong as the 2.5 in. main structural shells found in typical transport casks. In both cases, the main shell thickness is determined by the 6 in. puncture drop event. We are, therefore, qualitatively confident that the proposed DUCRETE cask system is able to meet the transportation structural criteria. Conservative manual calculations to support this are presented in the following sections.

3.1 Transportation Overpack

The transportation overpack is primarily responsible for withstanding the loads associated with the hypothetical 30 ft drop and 6 in. puncture events that transportation regulations require the cask system to withstand. The overpack spreads the loads associated with the corner drop and puncture events, and provides broad and even support for the DUCRETE storage cask and canister, limiting the stresses in those components. The overpack forms the containment boundary for the DUCRETE cask system, and the calculated stresses must be within the corresponding allowables. The overpack is also responsible for

containing its contents and roughly maintaining the DUCRETE material shielding geometry within the cask, so that dose rates do not greatly increase due to these events.

The overpack is required to withstand a 30 ft drop onto an unyielding surface at any angle. The impact limiters are assumed to be in place. The overpack must also withstand a 6 in. drop onto a 6 in. diameter steel pin, on the sidewall as well as on both ends. Drops onto the top and bottom cask corners are the limiting events that determine the required top and bottom plate thicknesses. The 6 in. puncture drop event determines the required thickness of the overpack shell. Given that the 2 in. thick overpack sidewall can withstand a 6 in. puncture drop, it is obvious that the much thicker end plates can survive this event as well.

In the following sections, calculations verifying the transportation overpack's adequacy with respect to the top corner drop, the bottom corner drop, and the 6 in. sidewall puncture drop events are presented. Calculations for the 30 ft side drop event are also presented to illustrate that the overpack also meets this condition.

3.1.1 Cask Side 6 in. Puncture Drop Event

This analysis considers the transportation overpack, with impact limiters, being dropped 6 in. onto a 6 in. diameter steel post. This drop event is illustrated in Figure 9. The Cask Designer's Guide⁶ gives a simple formula for determining the shell thickness required to withstand this event without puncturing, namely:

$$t = (w/s)^{0.71}$$

where t is the required shell thickness, w is the weight (in pounds) of the entire cask package (including impact limiters), and s is the ultimate strength of the material (in psi). This formula assumes that the main shell forms the containment boundary of the system.

The total system weight, as discussed in Section 6, is 132 tons, or 264,000 lb. The ultimate strength of XM-19 stainless steel is 99,500 psi. These parameters yield a required shell thickness of exactly 2.0 in., which is used in the proposed design.

3.1.2 Cask 30 ft Horizontal Drop

This analysis considers the loaded transportation overpack, with impact limiters, being dropped 30 feet onto an unyielding surface. The impact limiters are assumed to limit the peak acceleration to 44 g. Therefore, the analysis considers a case where the overpack is supported near its ends, by the impact limiters, and subjected to a 44 g horizontal body load. The bending (membrane) stress on the overpack shell is determined. A shell thickness of 2 in. is assumed. The 30 ft horizontal drop event is illustrated in Figure 10.

The membrane stress in the overpack shell from overall shell bending, f_b , for cylindrical systems is given by:⁷

M^*R/I ,

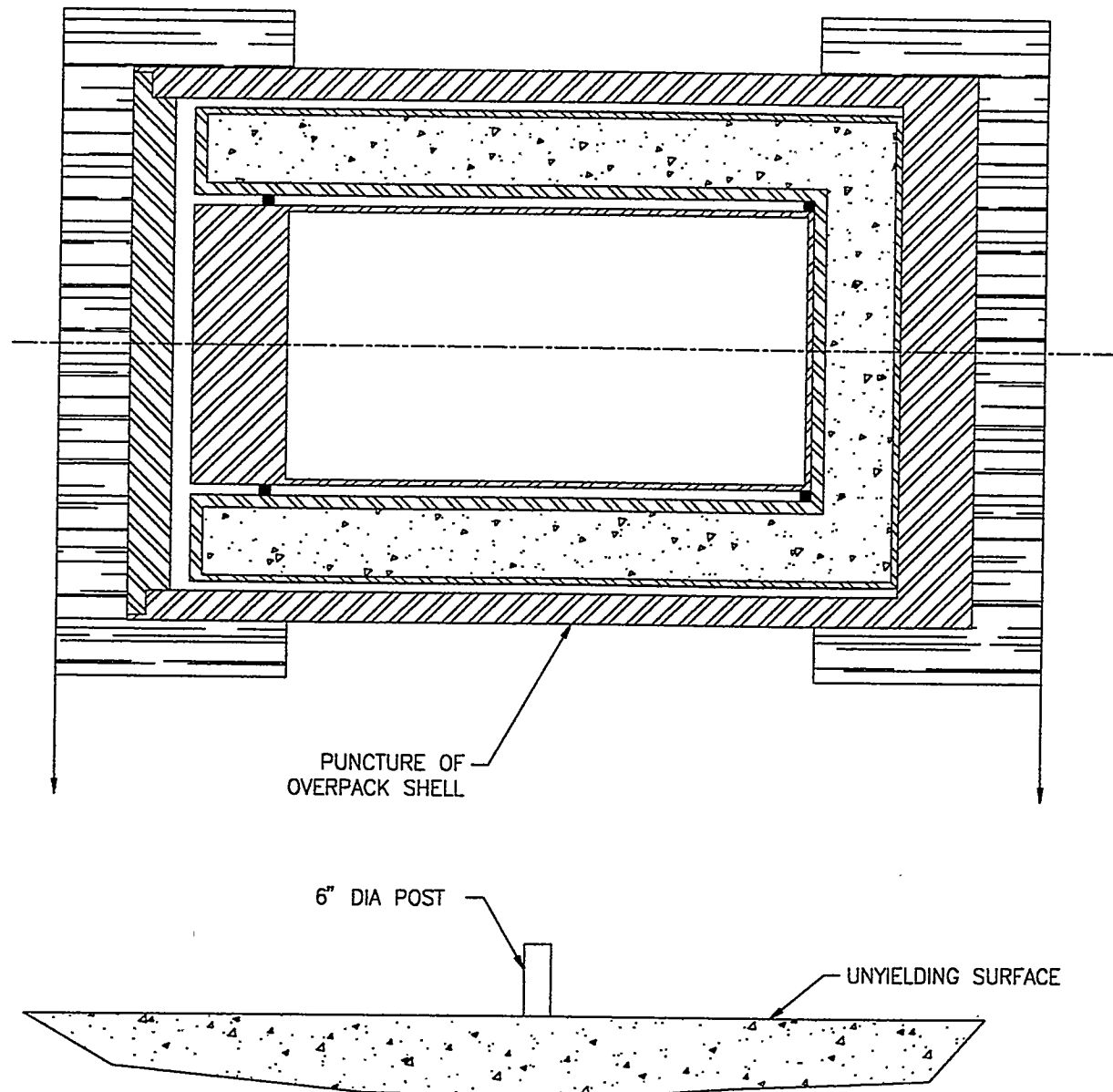


Figure 9. Puncture drop event—a 6 in. side drop onto a 6 in. diameter post. The overpack shell must be strong enough to resist puncture in this event.

where M is the bending moment, R is the overpack outer radius (47 in.), and I is the moment of inertia.

The bending moment, M , is given by:

$$M = 0.125 \times W \times A \times L$$

where W , total system weight, is 250,000 lb (125 tons); A , acceleration, is 44 g; and L , length between the end support points, is 202 in.

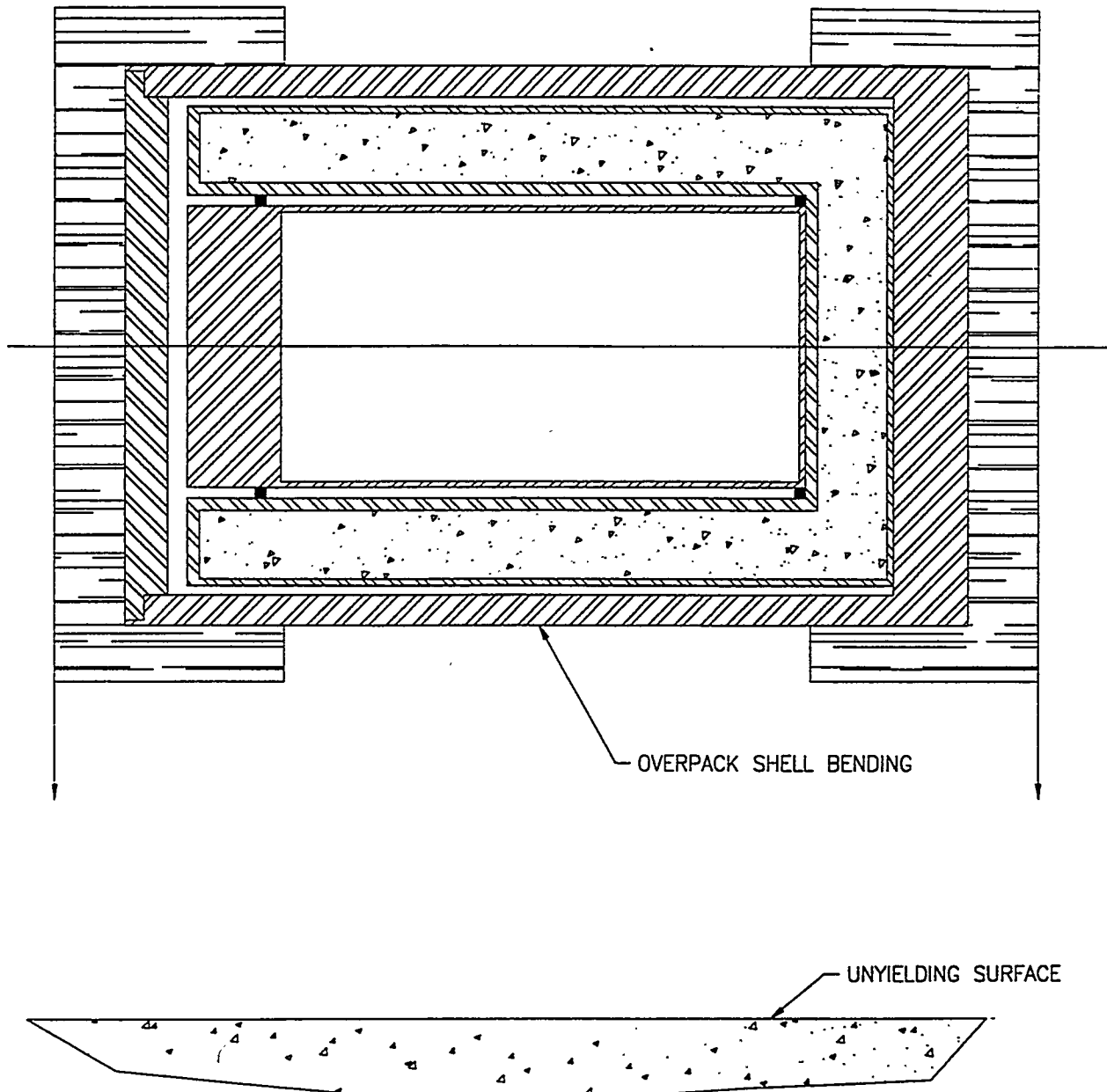


Figure 10. Cask side drop event—cask (with impact limiters) is dropped 30 ft onto a hard surface. This event causes bending stress in the overpack shell. These stresses must be under the ASME Code allowable stress level for containment boundaries.

In the horizontal drop, the cask is assumed to be supported by the impact limiters, so their weight is not included in the calculation. The maximum allowable overpack weight of 125 tons is conservatively assumed. The acceleration is assumed to be 44 g. The impact limiter sides extend 12 in. along the cask sidewall on each end. The point of support is assumed to be in the center of this 12 in. section, i.e. 6 in. from each cask end. Therefore, 12 in. is subtracted from the total overpack length of 213.75 in. to yield a length of 201.75 in., which is rounded to 202 in. Based on these values, the system moment, M , equals 2.7775×10^8 in-lb.

The moment of inertia, I , of the system is given by:

$$I = \pi (R_o^4 - R_i^4) / 4$$

where R_o and R_i are the outer and inner radii (in inches), respectively. The outer and inner radii of the overpack are 47 and 45 in., respectively. This leads to a moment of inertia equal to 611,689 in⁴.

With the values determined above, the calculated bending stress (M^*R/I) is equal to 21,341 psi ($2.7775e^8 * 47 / 611,689$). The yield strength of XM-19 stainless steel is 47,000 psi, the ultimate strength is 99,500 psi. The "design stress intensity", another allowable stress limit defined in the ASME Code, for XM-19 is 33,200 psi. ASME pressure vessel requirements for containment boundary materials state that the membrane stress must be under 2.4 times the design stress intensity of the material and under 0.7 times the ultimate stress of the material. The calculated maximum bending stress of 21,341 psi is under both limits by a more than a factor of three. The stress is only half the yield strength, so there is no permanent deformation of the overpack after a side drop event. Therefore, the 2 in. overpack shell thickness, which was set by the puncture requirement, is more than adequate to meet the 30 ft side drop criterion.

3.1.3 Cask 30 ft Drop onto Bottom Corner

This case considers the transportation overpack, with impact limiters, being dropped 30 ft onto an unyielding surface, with the point of impact being the bottom corner of the cask. In this event, the overpack shell comes to a stop and the bottom plate bears the weight of the overpack contents, i.e. the 96.5 ton loaded DUCRETE storage cask. This causes significant bending stresses in the bottom plate. This event determines the required thickness for the overpack bottom plate. The bottom corner drop event is illustrated in Figure 11.

The disk-shaped bottom plate is effectively supported at its edge. For the bottom plate, the disk edge is assumed to be fixed, not merely supported, since it is welded to the stiff overpack shell. Significant bending of this edge joint is assumed not to occur. The overpack contents are conservatively assumed to behave like a fluid, lending no structural support to the overpack bottom plate.

The angle of the cask is such that the cask center of gravity is directly over its bottom corner. The impact limiter corner regions are assumed to limit acceleration to 44 g during this event. The bottom end drop does not produce significant bottom plate stresses since the bottom plate is supported by the ground.

The angle of contact is equal to the arctangent of L/R , where R is the overpack radius of 47 in. and L is roughly half of the overpack length of 213 in., or 106.5 in. Thus, the angle is about 24 degrees.

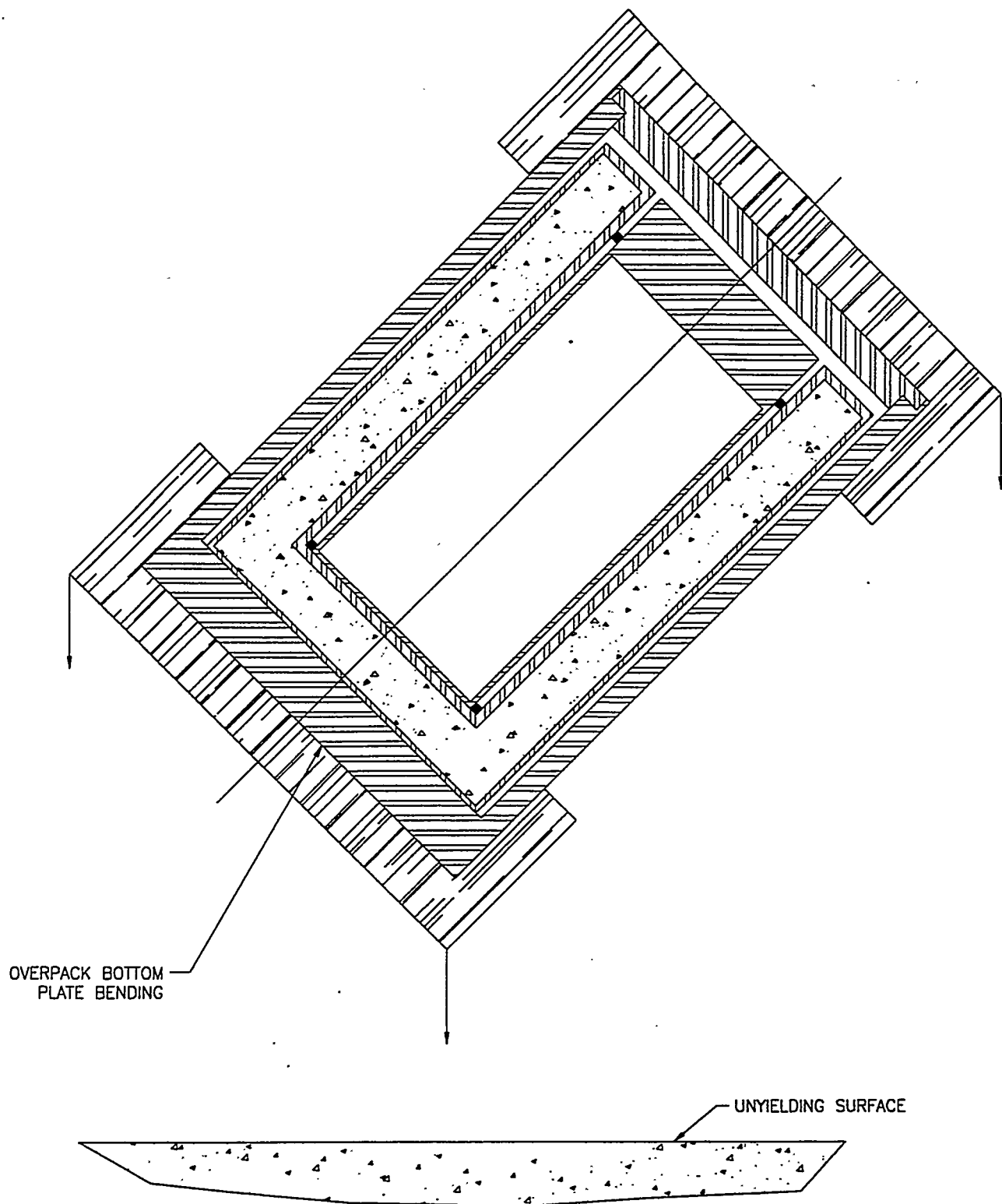


Figure 11. Cask bottom corner drop event—the cask system is dropped 30 ft onto its bottom corner on a hard surface. This creates bending stresses in the overpack bottom plate, which must be under the ASME containment boundary allowable stress level.

The formula used to calculate the maximum overall lower plate stress (bending plus membrane) is:⁷

$$S = 3*A*W_A/(4*\pi*t^2)$$

where W_A is the effective weight of the contents, A is the acceleration, and t is the plate thickness. The effective weight is equal to the actual DUCRETE storage cask weight times the cosine of the drop angle. The maximum allowable DUCRETE storage cask weight is 96.5 tons, or 193,000 lb. Thus the effective weight is $193,000 * \cos(24)$, which is 176,314 lb. The acceleration is 44 g.

The ASME containment boundary limits for overall stress (membrane plus bending) are 3.6 times the design stress intensity of the material or the ultimate strength of the material, whichever is lower. The design stress intensity for XM-19 is 33,200 psi. The ultimate strength is 99,500 psi. Therefore, for XM-19, the stress limit for overall bending is the ultimate strength of 99,500 psi.

For a stress limit of 99,500 psi, the above formula yields a required plate thickness is 4.314 in. Thus, the 4.5 in. plate thickness in the proposed design is adequate.

The maximum yield for the bottom plate is given by the formula:⁷

$$y = 3*A*W_A(m^2-1)a^2 / (16*\pi*E*m^2t^3)$$

where y is the total deflection in inches; m, for steel, is 3.333; a, the disk radius, is 45 in.; and E, Young's modulus for steel, is 30×10^6 psi. These values, along with the values for W_A , a, and t given above yield a total deflection of only about 0.3 in.

These calculations show that the overpack bottom lid meets containment boundary allowable stresses in a bottom corner drop. The calculations also show that the bottom plate does not undergo any significant deformation during the drop event. Therefore, it will contain the DUCRETE cask. For structural calculations, the cask can be considered to be inside a rigid body that transfers the g loads directly to the DUCRETE cask. The yielding of the overpack will not place additional loads on the DUCRETE cask.

3.1.4 Cask 30 ft Drop onto Top Corner

The top corner drop event is similar to the bottom corner drop event. In this case, bending stresses are created in the overpack top lid. This drop event is illustrated in Figure 12.

The top corner calculation is the same as the bottom corner drop calculation with two exceptions. First, the overpack top plate (lid) is 6 in. thick, as opposed to 4.5 in. for the bottom plate. Second, because the bolted closure does not provide as much support to the top lid edge as does the weld between the bottom plate and the cask shell, a different relation from Ref. 6 is used. This relation is for a disk whose edge is merely supported, not fixed, i.e.

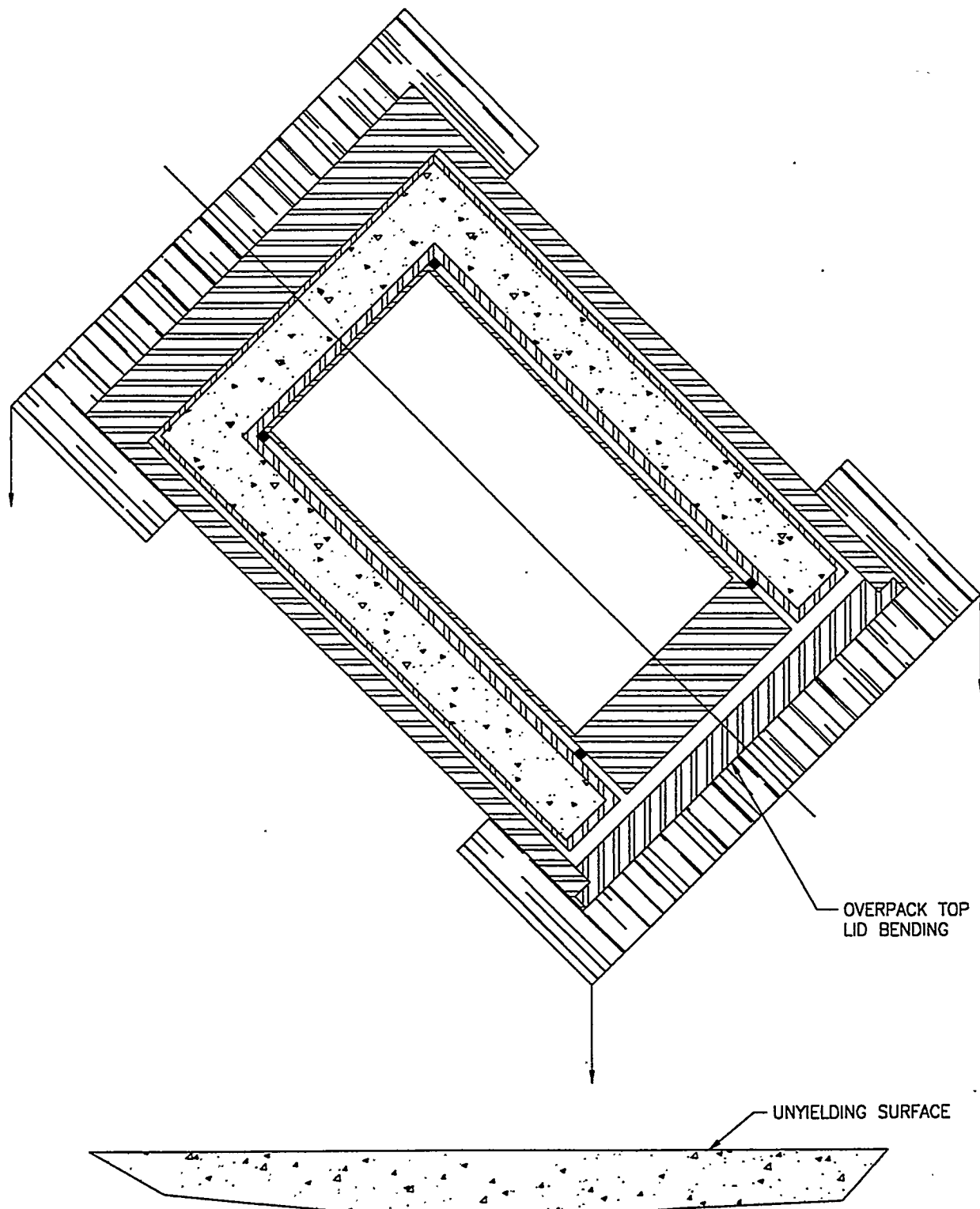


Figure 12. Cask top corner drop event—the cask is dropped onto its top corner on a hard surface, which creates bending stresses in the overpack top lid. These stresses must be under ASME containment boundary allowable stresses.

bending at the support location is allowed. With this relation, the overall top lid stress (in psi) is given by:

$$S = 3*A*W_A(3m+1) / (8*\pi*m*t^2)$$

where t , the lid thickness is 6 in. and, as in Section 3.1.3, $A = 44$ g, $W_A = 176,314$ lb, and $m = 3.333$. These values yield a maximum stress of 84,885 psi. This stress level is under the overall (bending plus membrane) stress limit for XM-19 stainless steel of 99,500 psi.

The total yield of the top lid is given by:

$$y = 3*A*W_A(m-1)(5m+1)a^2 / (16*\pi*E*m^2*t^3)$$

where $A = 44$ g, $W_A = 176,314$ lb, $m = 3.333$, $a = 45$ in., $E = 30 \times 10^6$, and $t = 6$ in. These values give a total yield of 0.54 in.

Thus, the calculations show that, as with the overpack bottom plate, the top plate meets containment boundary requirements for the top corner drop and does not undergo significant yielding. The DUCRETE cask can be considered to be inside a rigid body in the drop event. Also, the DUCRETE cask will remain confined inside the overpack.

3.2 DUCRETE Storage Cask

In transport mode, the internal canister is suspended inside the DUCRETE cask by two metal rings, one on each end of the ventilation duct. The cask is contained by the transportation overpack, which effectively is a rigid body with respect to the loads seen by the DUCRETE cask. The DUCRETE cask is not a containment boundary, it is a shield. The overpack protects the DUCRETE cask from puncture events and supports it in corner drop events. The main structural criteria that the DUCRETE cask must meet are to keep the inner canister from being crushed by DUCRETE during the drop events and to maintain its shape during ordinary lifting and moving operations at power plants, before it is placed in the transportation overpack. The DUCRETE is conservatively assumed to have absolutely no structural strength in these calculations. It only has mass and behaves like sand.

3.2.1 DUCRETE Cask Outer Shell Bottom Plate

The outer shell bottom plate, which forms the very bottom of the DUCRETE cask (as shown in Figure 3), must bear the weight of the DUCRETE when the cask is lifted. This normal operation case is actually the limiting case that determines the required plate thickness. During a bottom drop event, the plate is supported by the 4.5 in. thick overpack bottom plate, which is in turn supported by the ground. The overpack also supports the DUCRETE cask during corner drop events. During a top end drop, the plate must only support its own weight because the overpack bottom plate is self-supporting during this event. The simple cask lift event is illustrated in Figure 13.

The outer shell bottom plate does not bear the weight of the inner canister or of the DUCRETE cask inner shell during a lift. The inner shell supports the canister and is attached

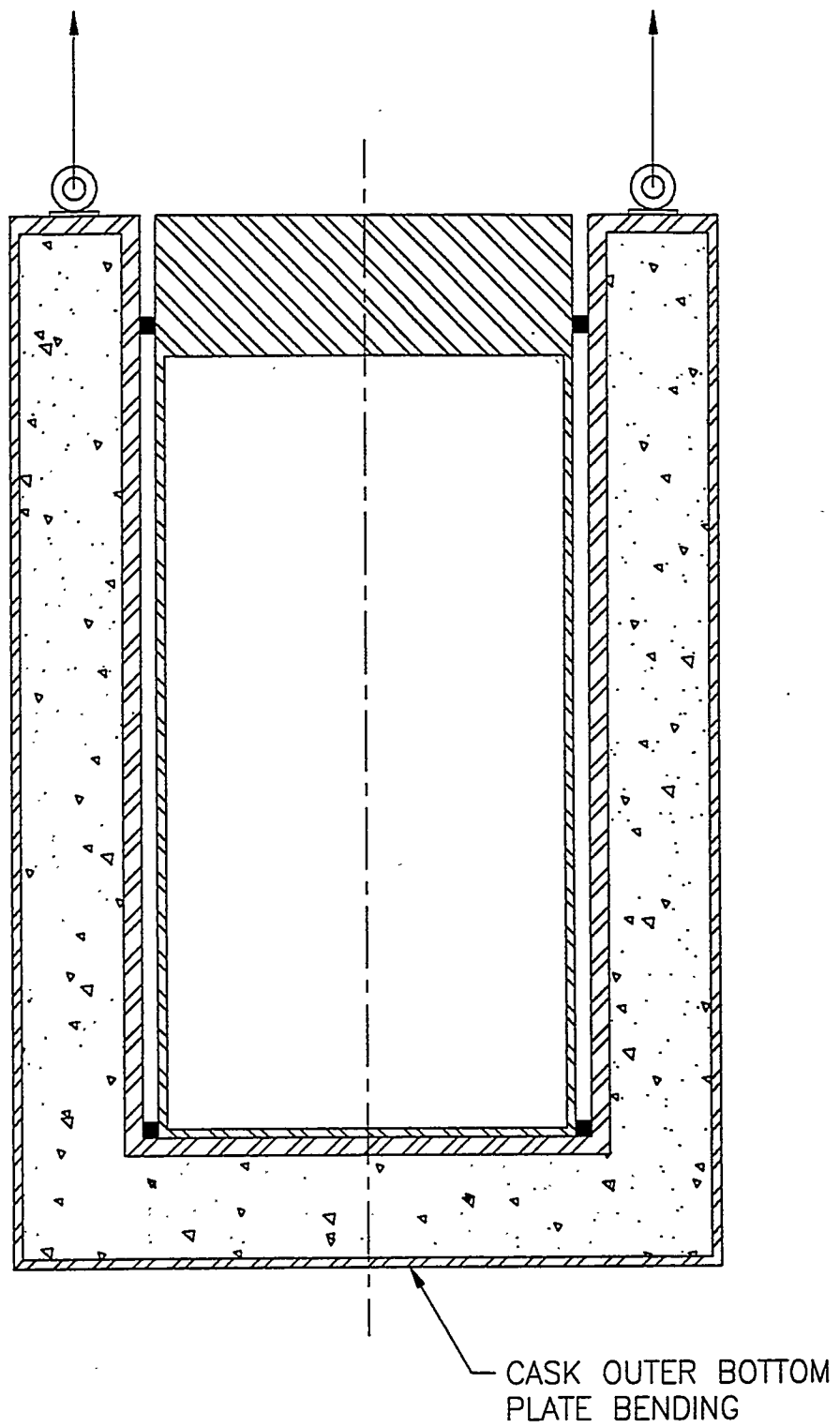


Figure 13. Normal condition lifting of DUCRETE cask—this condition creates bending stresses in the cask outer bottom plate. These stress levels must meet the requirements for normal system use.

to the DUCRETE cask flange where the lifting force will be applied. The inner shell can easily take the canister weight in tension and the inner shell bottom plate will take the canister weight without bending significantly. Also, if necessary, a support member could be run from the bottom corner of the inner shell to the bottom corner of the outer shell, which would relieve the bottom plate of the outer shell from any bending load from the inner shell and the canister.

There are two components to the outer shell bottom plate bending stress calculation. First, the plate must support its own weight plus that of the bottom disk of DUCRETE. Both disks are 44 in. in radius; the DUCRETE disk is 6 in. thick and the plate is 1.25 in. thick. The DUCRETE density is 0.1852 lb/in.³ and the bottom plate density is 0.284 lb/in.³. This leads to a total weight (DUCRETE + steel) of 8918 lb. The plate stress (assuming a fixed edge) is:⁷

$$S = 3*W / 4*\pi*t^2$$

where W, the disk weight, equals 8918 lb., and t, the plate thickness, equals 1.25 in. These values lead to an outer bottom plate stress of 1363 psi.

Second, the outer bottom plate must support the weight of the DUCRETE shielding material in the side of the DUCRETE cask. This column of DUCRETE extends from a radius of 34.625 in. to 44 in. and is 193.25 in. high. Its density is 0.1852 lb/in.³. The bottom plate stress is reduced, however, because this load will be applied near the edge of the bottom plate. The formula used above is also used to determine the stress on the bottom plate from the annular DUCRETE shield load. The stress from a complete cylinder of DUCRETE (r going from 0 to 44 in.) will be determined. Then, the stress from a smaller DUCRETE cylinder (r out to 34.625 in.) will be calculated and subtracted from the first stress. The remaining stress is due to the DUCRETE annulus (r from 34.625 to 44 in.).

The weight of a 193.25 in. high, 44 in. radius DUCRETE cylinder is 217,679 lb. Applying this weight and a plate thickness of 1.25 in. to the equation above yields a plate stress of 33,259 psi.

The weight of a 34.625 in. radius, 193.25 in. high DUCRETE cylinder is 134,800 lb. The stress in a plate bearing a load that does not go all of the way to the edge is given by:⁷

$$3*W*(1-r^2/2a^2) / (2*\pi*t^2)$$

where r = 34.625 in., a = 44.25 in., W = 134,800 lb, and t = 1.25 in. This yields a plate stress of 28,438 psi. The support point for the plate is assumed to be in the middle of the DUCRETE cask outer shell, at r = 44.25 in.

The second stress is subtracted from the first to yield a stress of 4821 psi (33,259 - 28438). This is the outer bottom plate stress from the annular column of DUCRETE. This stress is added to the stress calculated for the bottom DUCRETE disk and plus the bottom plate (1363 psi) to yield a total outer bottom plate stress of 6184 psi.

Normal use requirements are that the stress is no more than one third the yield strength of the material or no more than one fifth the ultimate strength, whichever is less. The yield strength of SA516 carbon steel is 33,700 psi and the ultimate strength is 70,000 psi. The stress is less than one fifth the yield strength and less than one tenth the ultimate strength of the material. Thus, the proposed thickness of the outer bottom plate is sufficient to meet the cask lifting load requirements.

During the top end drop, the outer shell bottom lid need only support its own weight. With a 44 in. radius and a 1.25 in. thickness, its weight is 2159 lb. The resultant stress is:⁷

$$S = 3*A*W / (4*\pi*t^2)$$

where A, the acceleration, is 124 g, W = 2159 lb, and t = 1.25 in. This yields a stress level of 40,907 psi, which is well under the carbon steel ultimate strength of 70,000 psi and just over the yield strength of 33,700 psi. Only a very small amount of plate yielding is expected during the top drop event. For this reason, the outer shell bottom plate weight will not bear on the inner shell bottom plate during the top drop event. Calculations will show that the inner shell bottom plate will yield more, since the stress will be much closer to ultimate.

3.2.2 DUCRETE Cask Inner Bottom Plate

The inner canister rests on the DUCRETE cask inner bottom plate (see Figure 3). It is above the bottom DUCRETE shielding when the cask is upright. This inner bottom plate is required to bear the load of the inner canister, without bending, during normal cask lifting operations. Also, it is required to support its own weight plus that of the cask bottom DUCRETE during the 30 foot cask top end drop event. The overpack bottom plate will easily support its own weight in a top end drop. Calculations show that the top end drop event, which is illustrated in Figure 14, determines the required thickness for the cask inner bottom plate.

The load borne by the inner shell bottom plate during the top end drop event is its own weight (that of a steel disk, 33.5 in. in radius and 1.5 in. thick), plus the weight of the bottom end DUCRETE shield (a disk of DUCRETE material, 33.5 in. in radius and 6 in. thick). Given the DUCRETE density of 0.1852 lb/in.³ and the steel density of 0.284 lb/in.³, the total load weight is 5420 lb. The acceleration during the end drop is 124 g. The stress formula is:⁷

$$S = 3*A*W / (4*\pi*t^2)$$

where A = 124 g, W = 5420 lb, and t = 1.5 in. These values lead to an inner shell bottom plate stress of 71,310 psi. This is very slightly over the ultimate stress of the material. The actual required thickness is 1.52 in. For simplicity, however, a thickness of 1.5 in. is assumed in the DUCRETE cask model. Given the conservatism of the formulas and approach, we are confident that a 1.5 in. thickness will be sufficient, especially since the structural strength of the 1 in. canister bottom plate has been neglected in this calculation.

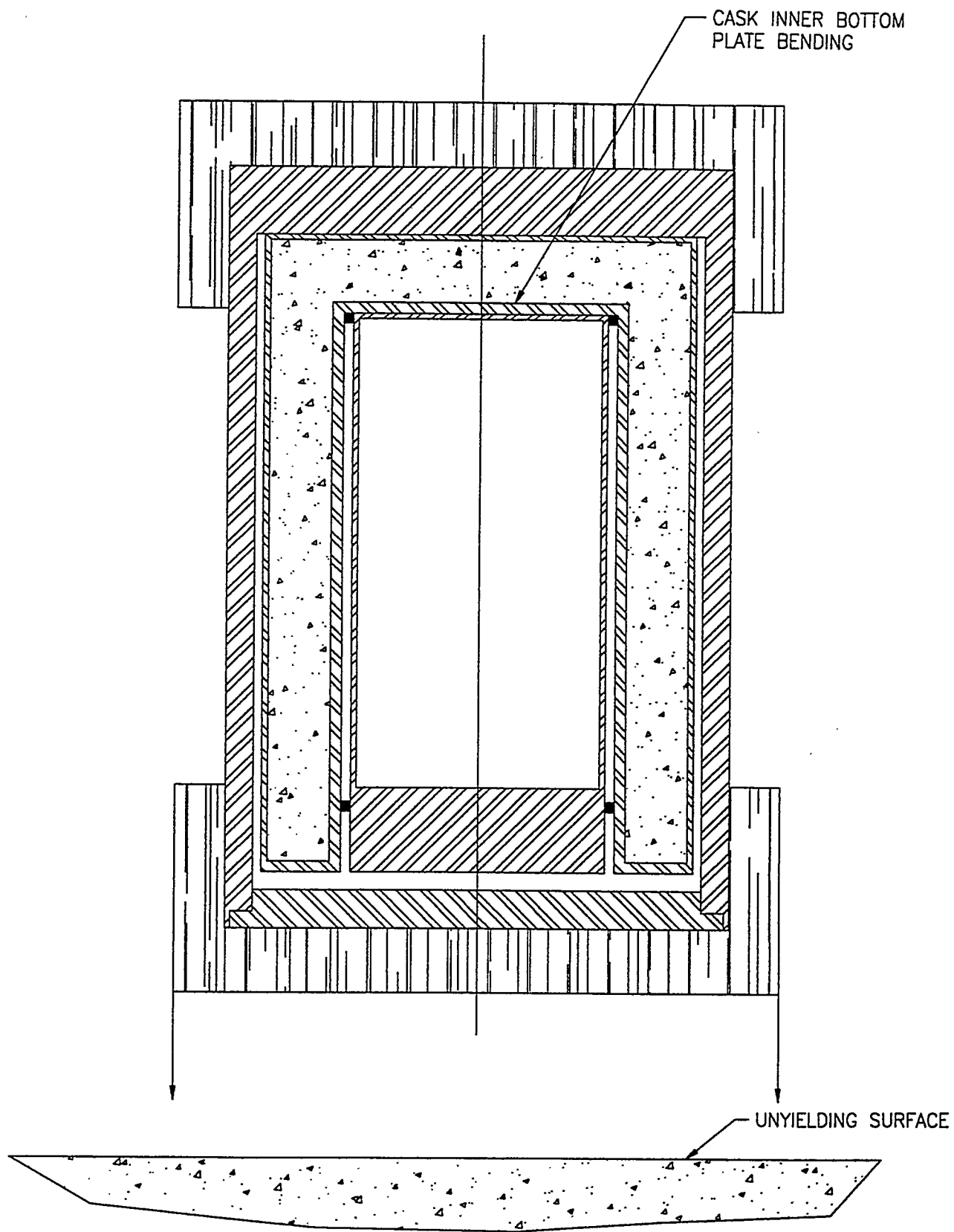


Figure 14. Cask top end drop event—cask is dropped 30 ft. onto its top end on a hard surface. This creates bending stresses in the cask inner bottom plate as it bears the weight of the bottom end DUCRETE shielding. The bottom plate must not yield enough to bear upon the canister.

The maximum deflection (yield) of the inner shell bottom plate during the top end drop is:⁷

$$y = 3*A*W*(m^2-1)*a^2 / (16\pi*E*m^2*t^2)$$

where $A = 124$ in.², $W = 5420$ lb, $m = 3.333$, $a = 33.5$ in., $E = 30 \times 10^6$, and $t = 1.5$ in. The resulting yield is ~0.6 in.

During the top end drop event the canister will be sitting on the overpack top lid. The overpack cavity is 0.5 in. longer than the DUCRETE cask. Thus, if the canister is sitting on the overpack top lid (when the cask system is upside down), the amount of space between its bottom plate and the DUCRETE cask bottom plate is 0.5 in. plus the difference between the DUCRETE cask cavity length and the canister length. The DUCRETE cask cavity will be slightly longer than the canister, although in this report they are assumed to be the same length. The above results show that only 0.6 in. of space will be required. It is, therefore, concluded that the 1.5 in. thick DUCRETE cask inner shell bottom plate is sufficient to meet the requirements of the top end drop event, namely to keep the weight of the DUCRETE material off the inner canister. The DUCRETE cask cavity, however, will have to be at least 0.1 in. longer than the canister unless more detailed structural calculations show that the deflection of the DUCRETE cask inner shell bottom plate is less than 0.5 in.

As stated before, the top end drop event determines the required cask inner bottom plate thickness. In a bottom drop, the plate may yield and the DUCRETE below it may crush, since this does not crush the canister. The canister must bear its own weight in a bottom end drop. Crushing the DUCRETE cask bottom end would actually reduce the acceleration that the canister sees and reduce its stresses. In actuality, the hydrostatic pressure of the DUCRETE would support the inner bottom plate in a bottom end drop. In corner drops, the DUCRETE, which is supported by the overpack, supports the DUCRETE cask inner shell.

The 1.5 in. plate thickness required for the top end drop event exceeds the requirements for normal cask lifting. In normal lifting, the inner canister is assumed to apply a uniform load over the inner 31.5 in. of the inner shell bottom plate. No credit is taken for the strength of the canister bottom plate or for any compressive strength of the DUCRETE below the inner shell bottom plate. The canister weight is assumed to be the maximum weight of 41 tons (82,000 lb). The edges of the inner shell bottom plate are assumed to be fixed by the DUCRETE cask inner side shell (no bending at the edge allowed). The following stress formula therefore applies:⁷

$$S = 3*W*(1-r^2/2a^2) / (2*\pi*t^2)$$

where the weight, W , equals 82,000 lb, the load radius, r , equals 31.5 in., and the plate radius, a , equals ~34 in., the mid-radius of the DUCRETE cask inner shell. If a plate thickness, t , of 1.5 in. is used, the resulting stress is 9932 psi.

The yield strength of SA516 carbon steel is 33,700 psi, so the calculated stress is only 0.295 times yield strength. It is required to be under one third of the yield strength. Also,

the ultimate strength of the carbon steel is 70,000 psi. The calculated stress is only one seventh of this value; it is required to be under one fifth of the ultimate strength. Therefore, the DUCRETE cask inner shell bottom plate is sufficient to meet the cask lifting load requirements.

3.2.3 DUCRETE Cask Inner Shell

The DUCRETE cask inner shell must keep the weight of the DUCRETE off the inner canister during the 30 ft cask drop events. Given that the DUCRETE is considered to have no structural strength and thus behave like sand, a large hydrostatic pressure bears on the inner shell during the 124 g cask end drop events. This stress turns out to be much larger than the bending stress placed on the inner shell by the DUCRETE during the 40 g horizontal drop event. Thus, the "slumping" effect determines the thickness of the DUCRETE cask inner shell. The bottom end drop event is illustrated in Figure 15.

The equation for determining the hydrostatic pressure from the DUCRETE on the bottom portion of the cask inner shell is:⁸

$$P = k * \rho * h * A$$

where ρ is the DUCRETE density, h is the height of the DUCRETE shield above the point at which the pressure is being calculated, A is the acceleration level, and k is a factor, taken from Reference 8, that adjusts the pressure based upon the medium's characteristics. For water, this factor is 1.0. For a sand-like material, the factor is 0.22. The DUCRETE density is 0.1852 lb/in.³. As shown in Figure 3, the vertical distance between the top edge of the inner shell bottom plate (i.e. the bottom of the inner side shell) and the top edge of the DUCRETE material is 191.75 in. The peak acceleration for cask end drop events is 124 g. These values lead to a hydrostatic pressure of 968.8 psi.

Roark⁷ gives a formula for how much external hydrostatic pressure a metal cylinder can withstand before collapsing. The collapsing pressure is given by:

$$P_c = 0.807 * (E * t^2 / L * R) * [(1 / (1 - v^2))^3 * (t^2 / R^2)]^{1/4}$$

where $E = 28.3 \times 10^6$ psi (for carbon steel), $t = 1.125$ in., $L = 191.75$ in., $R = 34$ in. (the average shell radius), and $v = 0.3$ (for steel).

These values yield a collapsing pressure of 865.6 psi, somewhat under the hydrostatic pressure of 968.8 psi determined above. To make the collapsing pressure equal 968.8 psi, a slightly higher thickness (1.177 in.) must be used.

Since hydrostatic pressures in excess of the collapsing pressure only exist along the bottom 10% of the inner shell (Roark's formula is based upon the pressure being applied along the entire cylinder length), it is thought that formal analyses will show that the design thickness of 1.125 in. will be sufficient. In any event, raising the inner shell thickness from 1.125 in. to 1.177 in. (less than a 5% increase) will have no significant effect on the shielding or thermal analysis results, or on the cask weight (it adds only ~200 lb.).

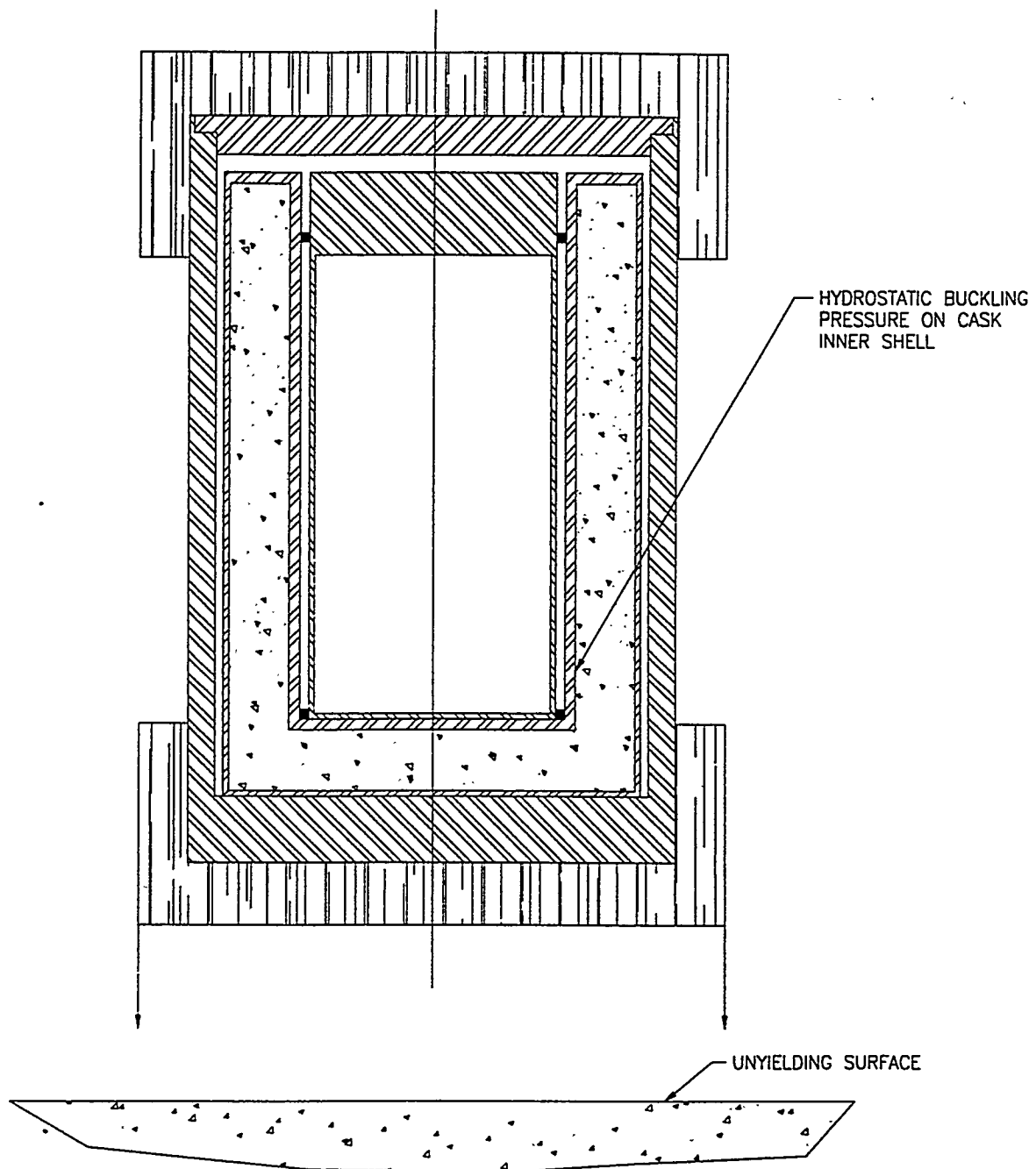


Figure 15. Cask bottom end drop event—cask is dropped 30 ft onto its bottom end on a hard surface. During this event, the DUCRETE material exerts a large hydrostatic pressure on the cask inner shell. The inner shell must withstand this pressure without failing (bursting).

3.2.4 DUCRETE Cask Outer Shell

There are no stringent structural requirements on the DUCRETE cask outer shell. The shell must be able to bear the cask weight (in tension) during cask lifting. But dividing the maximum loaded cask weight (200,000 lb) by the 0.5 in. thick shell's area of 139 in.² yields a stress of only 1440 psi, a factor of 23 below the yield strength. In drop events, the DUCRETE cask outer shell is allowed to fail. The 2 in. thick XM-19 overpack shell is easily able to take the pressures and loads from the DUCRETE. The DUCRETE material may collapse outward without crushing the internal canister. Thus, the only serious requirements are on the cask's inner shell.

3.3 Inner Canister

The inner canister forms an additional (redundant) containment boundary for the DUCRETE cask system in transport, with its two, redundant, lid seal welds providing containment. The canister is protected by the transportation overpack from all external localized blows during the drop and puncture events. The DUCRETE cask structure supports the weight of the DUCRETE material, keeping it from bearing on the canister walls during drop events. During corner drops, the overpack structure, the DUCRETE hydrostatic pressure, and the DUCRETE cask inner shell structure support the corner of the canister. Basically, during the drops, the cavity that the canister is in is assumed to be a rigid body with respect to the canister's structural calculations.

The internal canister must support its own weight without buckling during cask top and bottom end drop events. Also, the canister may be lifted as part of a canister transfer operation, so the bottom plate must be able to bear the weight of the canister and its contents. The inner canister must meet these criteria, however, whether it is in the DUCRETE cask system or a standard transportation cask. Since the accelerations assumed in the DUCRETE cask analyses are those typical of transport casks, and in both cases the canister is inside a rigid cavity, the requirements on the canister are the same. Since it can be assumed that the MPC system canister will be designed to meet these criteria, they will not be studied here. Therefore, the DUCRETE cask system canister analyses focus solely on the only major difference between the DUCRETE system and a standard transportation cask system, the steel rings supporting the canister.

In a standard transportation cask system, the internal canister is inside a smooth cylindrical cask cavity. A radial gap of about 0.5 in. exists between the canister and the cask. In the DUCRETE system, a 2 in. thick ventilation duct exists between the canister and the DUCRETE storage cask inner shell. The canister is not permitted to "roll around" inside this large space—it is suspended in the middle of the cask cavity by two steel rings, one near the top and the other near the bottom of the cavity (see Figure 3). The rings are about 180 in. apart. With a standard cask system, in a side drop event the canister is well supported by the cask inner shell. With the DUCRETE cask system, the canister shell must bear the bending stresses associated with being supported only by its ends during the 40 g cask side drop event. This drop event is illustrated in Figure 16.

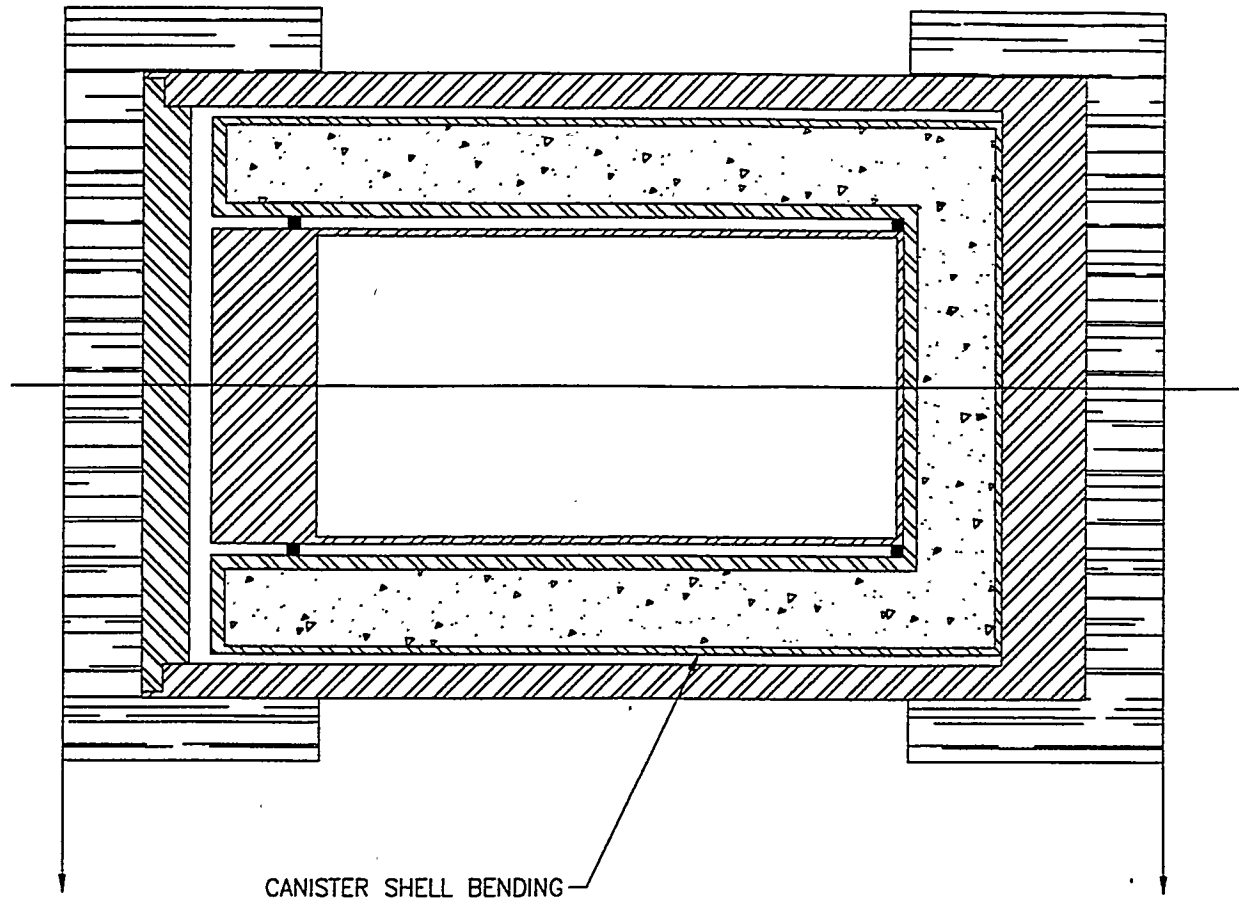


Figure 16. Cask side drop event (same as that shown in Figure 10)—this event also creates bending stresses in the inner canister shell, since the canister is supported at its ends by the canister support rings. This creates bending stresses in the canister shell. Although the canister is not a containment boundary, the bending stresses meet ASME containment boundary criteria.

The bending stress, f_b , in the canister wall is given by the formula:⁷

$$f = M * C / I$$

where M is the canister's bending moment, C equals the outer radius of the canister, and I is the moment of inertia of the canister shell. The bending moment is given by the formula:

$$M = 0.125 * W * A * L$$

where W , the canister weight, is conservatively assumed to be the maximum (dry) value of 75,000 lb (37.5 tons); A , the peak acceleration, is 44 g; and L , the distance between the support rings, is ~ 184 in. (the distance between the two support ring centers). Thus, the bending moment is 7.59×10^7 in.-lb. The moment of inertia is given by:

$$I = \pi^* (R_o^4 - R_i^4) / 4$$

where R_o , the outer radius of the canister shell, is 31.5 in. and R_i , the inner radius of the canister shell, is 30.75 in. These values lead to a moment of inertia of 71,056 in.⁴.

The bending moment and moment of inertia calculated above yield a bending stress of 33,647 psi. As mentioned in Section 3.1.2, ASME defines a design stress intensity allowable. For Type 304L stainless steel, this allowable is 16,700 psi. ASME pressure vessel standards allow stresses of 2.4 times the design stress intensity or 0.7 times the ultimate stress limit, whichever is lower. The ultimate strength of 304L is 60,900 psi. These two criteria produce stress limits of 40,080 psi and 42,630 psi, respectively. The bending stress in the canister for the DUCRETE system meets both of these criteria.

As mentioned before, the canister will also be designed meet the structural requirements for transport inside standard shipping casks. Sierra Nuclear has performed calculations² showing that the VSC canister can withstand the 124 g drop events without buckling. Preliminary calculations show that an MPC canister with a 0.75 in. 304L stainless steel shell can also meet the requirements. Calculations for SNC's proposed MPC canister indicate that a 1 in. thick stainless steel bottom plate will be required to meet the canister lifting loads. For this reason, those canister shell and plate dimensions are assumed in the DUCRETE thermal and shielding analyses.

4.0 THERMAL EVALUATION

Computational thermal analyses have been performed for the DUCRETE storage cask inside the steel transportation overpack. The system is explicitly modeled by the two-dimensional, azimuthally-symmetric, ANSYS model; the mesh used is shown in Figure 8. Details of the geometry, material properties, and analysis methodology are presented in Section 2 of this report. A brief review of the key assumptions made in all of the analyzed cases is presented below.

The model is based on the geometry shown in Figure 3 and the material properties given in Table 3. A heat load of 17.52 kW inside the internal canister is assumed. Axial peaking of the heat generation is modeled, with the peak generation level being about 30% higher than the average level. This heat source resembles that specified in the MPC system specification. Convection in voids and gaps in the system geometry is conservatively neglected. An emissivity of 0.8, that of unpolished metal, is assumed for all metal surfaces in the cask system except the overpack exterior, which is assumed to be coated with white paint and have an emissivity of 0.9. The overpack does not go into the spent fuel pool. The overpack surface solar absorbtivity is assumed to be 0.3. The solar insolation level is assumed to be about 780 W/m². The solar heat load is applied evenly over the overpack's cylindrical side surface.

The overpack surface is cooled by natural convection as well as radiation. Natural surface convection coefficients of 0.65 Btu/hr-ft²-°F (for the overpack ends) and 0.75 Btu/hr-ft²-°F (for the overpack side) are applied to the overpack outer surface. The ambient air temperature is assumed to be 100°F. In some cases, fin structures are used. In these cases, the fin structure is modeled by an enhanced surface convection coefficient over that section of the overpack surface. The fin structure would also increase overall radiation from the overpack surface due to the increase in the effective area. However, the thermal analyses conservatively ignore this effect.

The 2 in. ventilation duct is modeled as dead air space—when the cask is in the overpack, all ventilation is cut off. A 0.5 in. gap is assumed to exist on all sides (side, top, and bottom) between the DUCRETE cask and the overpack.

The ANSYS models are not used to determine the temperatures inside the inner canister. Rather, the ANSYS models fill the canister with a simple homogenized material with an effective conductivity that approximates the canister interior's temperature profile. If the effective axial conductivity of the interior is correct, this treatment will not cause any inaccuracy in temperatures outside the canister interior.

As discussed in Section 2.3, the canister interiors were analyzed by making minor modifications to detailed canister interior thermal models that were developed for the VSC system canister. The modifications reflect the horizontal orientation of the canisters and the differences between the MPC canister and the VSC system canister. Two runs, one which models the VSC canister, and one which models the MPC system canister, were performed to calculate the difference between the peak canister shell temperature and the maximum fuel

clad temperature. Then the results from the canister interior models were used to determine peak clad temperatures for each case.

4.1 Analyzed Cases

4.1.1 Base Case

The ventilation duct and the system gaps are assumed to be filled with helium. A 144 in. section of the overpack's outer surface, the section over the active fuel region, is assumed to be covered with an extensive annular fin structure for heat transfer. This fin structure is modeled using an enhanced surface convection coefficient of 2.5 Btu/hr-ft²-°F over that section of the overpack surface. (This represents a factor of 3.333 enhancement over the 0.75 Btu/hr-ft²-°F coefficient that would be present without the fins.)

A large set of aluminum fins, 2 in. long, 0.125 in. thick, and spaced 0.5 in. apart, would increase the effective area of the overpack surface by a factor of ~5. The overall enhancement in surface convection is equal to the increase in effective area times the "fin efficiency factor", which accounts for temperature differences between the base of the fins (and the shell surface) and the fin tips. Formulas⁵ predict a fin efficiency factor of about 2/3 for the set of aluminum fins described above. This yields an overall increase in surface convection of about 3.333 (5 x 2/3). Thus, the proposed fin structure is roughly predicted to produce the effective surface convection coefficient assumed in the base case ANSYS analysis.

Aluminum must be used for the fin structure due to its low weight and its very good thermal conductivity—carbon steel has about three times the density and only one third the conductivity of aluminum. Given that only a fixed amount of "spare" weight is available for a fin structure, if steel were used, only ~1/3 the number of fins could be used, greatly reducing the increase in effective area. Also, due to the reduced conductivity of steel fins, the fin efficiency would be significantly reduced. This means that a way of bonding the aluminum fins to the stainless steel structure must be found. It is proposed to clad (or bond) a 1/8 in. aluminum coating onto the overpack surface. Experience has shown that this can be done. The fins would be welded to this aluminum coat.

The base case model assumes an effective thermal conductivity of 2.5 Btu/hr-ft-°F for the DUCRETE material region. This effective conductivity is based upon a DUCRETE conductivity of ~1.2 Btu/hr-ft-°F, which is based on preliminary theoretical calculations performed at INEL.⁷ An additional 1.3 Btu/hr-ft-°F of effective thermal conductivity is assumed to be added due to presence of a heat transfer fin structure that extends between the DUCRETE cask inner and outer shells. This conductivity enhancement is based upon a set of 36 0.5 in. thick radial carbon steel fins, about seven in. apart, extending between the carbon steel cask shells. The fins are assumed to be welded at both ends, giving perfect thermal contact with the shells. If the shells had perfect heat conductivity, the effective fin conductivity would be the carbon steel conductivity of 26 Btu/hr-ft-°F times the fin area fraction of 0.07287, which yields an additional conductivity of 1.895 Btu/hr-ft-°F.

A simple average heat conduction path method is used to estimate the reduction in fin effectiveness due to temperature distributions through the shells. The "average" heat conduction path length is about 1.5 in. through the 1.125 in. thick inner shell, 9.375 in. through the 0.5 in. fin, and about 2 in. through the 0.5 in. outer shell. This leads to an overall conduction path resistance that is 28% higher than that of just the fin segment of the conduction path. This leads to a fin effectiveness of 0.78 times the ideal value and an effective conductivity of 1.4781 Btu/hr-ft-°F (1.895 x 0.78). To determine the overall conductivity of the DUCRETE region, the DUCRETE conductivity of 1.2 Btu/hr-ft-°F is multiplied by (1 - 0.07287) and added to the fin conductivity of 1.4781 Btu/hr-ft-°F. This yields an overall DUCRETE region conductivity of 2.59 Btu/hr-ft-°F, showing that the proposed carbon steel fin structure would produce the effective DUCRETE region thermal conductivity of 2.5 Btu/hr-ft-°F assumed in the ANSYS analyses.

The fin design given above may not be the one finally used. Welding all of the fins may be too expensive. Instead, the design may rely on aluminum fins that are merely inserted between the two shells. The increased heat conductivity of the fins would offset the effects of imperfect thermal contact between the fins and the shells. Also, aluminum fins would reduce cask weight, possibly allowing more shielding. The ANSYS model does not specify a fin design, but merely an effective conductivity. At a later time, fin structures will be designed with a specific effective conductivity goal, based on the ANSYS results. The carbon steel arrangement described above was studied because one can calculate the effective conductivity and that system is known to work. Accurately estimating the effective conductivity of an imperfect contact system would be difficult.

4.1.2 Alternative Cases

A number of alternative cases were studied along with the base case. As there are still many unanswered engineering and scientific questions associated with the DUCRETE material and the DUCRETE cask design, alternative analyses must be performed to evaluate the effect of changing various assumptions made in the base case.

Three additional ANSYS runs that assume different DUCRETE region effective conductivities were performed because it is not clear what the actual conductivity of the DUCRETE material will be. The conductivity is thought to depend on the DUCRETE composition, but the optimum composition (from a cask design perspective) has not been established, and composition will vary somewhat from cask to cask. Also, it is not clear whether a heat transfer fin structure between the cask shells will be economical or practical.

In response to these uncertainties, ANSYS analyses of a wide range of DUCRETE region thermal conductivities are presented. In the formal design phase, when the effective conductivity is known, temperatures can be estimated by interpolating between the data (temperatures) presented in this report.

The lower bound DUCRETE region conductivity is 0.72 Btu/hr-ft-°F, the conductivity of ordinary concrete with no fin structure. Since UO_2 pellets have a higher conductivity than ordinary gravel, DUCRETE is known to have a conductivity higher than concrete, but it is not clear how much higher it will be. Another case assumes a DUCRETE region conductivity of

1.2 Btu/hr-ft-°F, the theoretical DUCRETE conductivity estimate from Reference ?. This case, therefore, assumes a "best guess" DUCRETE conductivity value, but no fin structure. The base case, as mentioned in Section 4.1.1, assumes a DUCRETE region conductivity of 2.5 Btu/hr-ft-°F, which is based upon the best guess DUCRETE conductivity and the fin arrangement that was described. Finally, the upper bound case assumes a hypothetical DUCRETE region conductivity of 5.0 Btu/hr-ft-°F. This involves a hypothetical fin arrangement that adds an additional 3.8 Btu/hr-ft-°F of effective conductivity, three times the amount of the base case fin arrangement. This clearly represents the upper bound on the effectiveness of any practical fin structure.

Another alternative case studied assumes the gap between the DUCRETE cask and the transportation overpack is filled with water to reduce the temperature drop across the gap and, therefore, reduce the DUCRETE temperatures. In this case, the DUCRETE cask inlet and outlet ducts would be sealed before shipment. The cask would be placed in the overpack. Then the gap between the cask and the overpack would be filled with water before the lid of the overpack is bolted on. A small void volume could be left to accommodate water expansion without significantly affecting the effective conductivity of the water sheath. In this case, the ventilation duct is assumed to be filled with air, as opposed to helium, since there are no ports through which to pump helium into the ventilation duct after the overpack lid is sealed. Initial estimates show that temperatures in the water sheath will not exceed water's boiling point.

Another case studies the system temperatures without the extensive fin array on the overpack surface. In this case, the surface convection coefficient that is applied to the 144 in. fin area of the overpack surface in the base case is simply reduced to 0.75, the bare cylinder coefficient.

Finally, the DOE may require an electro-polished surface for the DUCRETE cask outer surface, if it is to be fully compatible with the MPC system. The MPC specification requires such a surface for all cask system components that are "routinely wetted" with fuel pool water. The DUCRETE cask is placed in the pool only once, but the cask outer shell must be decontaminated. DOE's interpretation of "routinely wetted" is unclear in this case. The VSC system transfer cask surface has a primer coating. Experience has shown that these coatings have a high level of decontaminatability and an emissivity similar to painted coatings (> 0.9). Therefore, we are reasonably confident that a coating with an emissivity of at least 0.8, as assumed in the base case thermal analysis, will provide acceptable decontamination performance. However, if the DOE requires an electro-polished cask outer surface, the emissivity would fall to ~ 0.2 . Therefore, an ANSYS run with the DUCRETE cask wall emissivity set to 0.2 was performed. Lowering the emissivity reduces the radiative heat transfer between the DUCRETE cask and the overpack by a factor of four. However, if the gap between the DUCRETE cask and the overpack is filled with water, as is done in one of the alternative cases, the DUCRETE cask emissivity has no effect on the thermal performance of the system.

Table 7 summarizes the cases that were thermally analyzed with the ANSYS code. For each case, the values of the parameters that were varied are listed.

Table 7. DUCRETE Cask ANSYS Model Parameter Summary.

	Case 1 ^a	Case 2	Case 3	Case 4	Case 5	Case 6	Case 7
DUCRETE Region Conductivity (Btu/hr-ft-°F)	2.5	0.72	1.2	5.0	2.5	2.5	2.5
Overpack Fins Present ?	Yes	Yes	Yes	Yes	No	Yes	Yes
DUCRETE Cask Surface Emissivity	0.8	0.8	0.8	0.8	0.8	N/A	0.2
Cask/Overpack Gap Fill	He	He	He	He	He	H ₂ O	He
Ventilation Duct Gas	He	He	He	He	He	Air	He

a. Case 1 is the base case ANSYS analysis.

4.2 ANSYS Thermal Analysis Results

4.2.1 ANSYS Results

The key results of the ANSYS analyses are the peak temperatures for each cask sub-component. These generally occur on the inner surface of the component, roughly over the axial center of the fuel region where the peak fuel heat generation occurs. The peak temperatures, presented in Table 8, are taken directly from ANSYS output except for the peak fuel clad temperature, which is calculated as discussed in Section 2.3.2.

The ANSYS run that models the MPC canister interior (discussed in Sections 2.3 and 4.0) predicts a 242°F temperature difference between the peak fuel clad temperature and the peak canister wall temperature, based on a heat load of 17.52 kW. The VSC system canister interior model predicts a temperature difference of about 325°F, based the same heat load.

4.2.2 Discussion of Results

The base case results give a peak DUCRETE temperature of 275°F and a peak fuel clad temperature of 607°F. The cladding temperature limit is under the 644°F limit set in the MPC Specification.³ The larger question is what the maximum permissible DUCRETE temperature will be; this will be the subject of further laboratory work at INEL.

As stated in Table 8, the estimated peak fuel clad temperatures for the VSC system canister, if the same 17.52 kW heat load is assumed, are about 100°F higher than those calculated by ANSYS for the MPC canister. The 644°F limit was not developed for a canister transportation system, it is the long term storage temperature limit for fuel that is 10 years cooled when placed in storage and is based upon a 0.5% chance of fuel rod failure over a 40 year storage period. The short term limits are much higher, over 1000°F. However, the MPC Specification requires that the long term (storage) temperature limit be applied to fuel being transported in the MPC system.

Table 8. Peak Temperatures (°F) for DUCRETE Cask System Components

	Case 1 (Base Case)	Case 2	Case 3	Case 4	Case 5	Case 6	Case 7
	Conductivity $y = 2.5^a$	Conductivity $y = 0.72$	Conductivity $y = 1.2$	Conductivity $y = 5.0$	No Fins	Water in Gap	Electro- polished
Transport							
Overpack Surface	154	151	153	154	193	155	154
DUCRETE Cask							
Outer Shell	202	196	199	202	236	180	214
DUCRETE Shield	275	427	345	239	308	253	287
DUCRETE Cask							
Inner Shell	276	428	346	240	309	254	288
Inner Canister							
Shell	365	485	418	339	390	369	374
Fuel Cladding ^b	607	727	660	581	632	611	616

a. DUCRETE conductivity in Btu/hr-ft-°F.

b. Based on MPC canister. VSC canister will produce temperatures ~100°F higher.

There are many criteria in the MPC specification that the VSC canister does not meet. The goal is not to make the VSC canister meet all of these specifications, but to (potentially) license it for transportation in the DUCRETE system or some other system. In any event, the VSC canister will not be required to meet the 644°F limit set specifically for the MPC canister. Instead, it will only have to meet the standard short term fuel temperature limits, which are several hundred degrees over the temperatures calculated in this report. Therefore, for the VSC canister, fuel cladding temperature limits are never a concern.

Examining the results shown in Table 8, the peak DUCRETE temperatures vary strongly with the conductivity of the DUCRETE region. The VSC system SAR² gives a long term peak concrete temperature limit of 225°F, and a short term limit of 350°F. At best, DUCRETE is expected to be as strong as concrete in this regard and it may be somewhat weaker.

Based on these facts, if DUCRETE only has the conductivity of concrete (Case 2 in Table 8), unacceptable temperatures will result unless heat transfer fins through the DUCRETE region are used. If DUCRETE's conductivity is roughly equal to that of early theoretical estimates (Case 3 in Table 8), then DUCRETE temperatures approach the most optimistic upper bound, 350°F. Note that the fuel clad temperature limit for the MPC canister (644°F) is exceeded roughly at the same conductivity level at which the DUCRETE material approaches its absolute upper bound limit. For this reason it is fair to say that the DUCRETE material temperature limit is the limiting constraint on the required thermal performance (or

the maximum allowed heat source) for the DUCRETE cask system in transport mode. Even if the DUCRETE temperature limit turns out to be 350°F, the DUCRETE limit and the fuel clad limit are met roughly simultaneously.

The base case yields a peak DUCRETE temperature of 275°F, which has a much greater chance of being acceptable for transportation (i.e. short term). The high conductivity case (Case 4) yields a peak DUCRETE temperature of only 240°F, which is very likely to be acceptable over a short term.

Case 5 shows that removing the fins from the cask overpack increases the overpack surface temperature significantly, by ~40°F. This temperature increase adds to the rest of the system temperature for the most part. The effect fades somewhat as one moves inward due to increased radiative heat transfer and axial conduction. The peak DUCRETE temperature rises by 33°F, and the peak clad temperature rises by 25°F, remaining under the fuel clad temperature limit.

Case 6 shows that filling the gap between the transportation overpack and the DUCRETE cask with water, as opposed to helium, reduces the DUCRETE cask outer surface temperature by over 20°F. The peak DUCRETE temperature falls by the same amount. There is no benefit in the peak clad temperature, however, because using air in the ventilation duct instead of helium causes the temperature drop across the duct to increase by about 20°F, cancelling the initial benefit of the water in the cask/overpack gap. Thus, the fuel clad temperatures turn out to be roughly the same as in the base case.

Case 7 shows that a polished DUCRETE cask outer shell increases system temperatures by about 10°F. This increase occurs throughout the system.

4.3 Maximum Heat Loads for DUCRETE Cask Systems

4.3.1 Estimated Cask Temperatures vs. Heat Load

As discussed in Section 4.2.2, the DUCRETE material temperature limit will be the limiting factor on the heat load that can be accommodated by a DUCRETE cask system. Since the DUCRETE temperature limit has not been established, it is not possible at this time to establish a DUCRETE cask design thermal performance level or a heat load limit. It is possible, however, to calculate a maximum permissible heat load as a function of maximum allowable DUCRETE temperature. Maximum heat load can be plotted versus the maximum temperature for various cask designs or configurations.

There is a simple method for approximating system temperatures versus heat load that will yield temperatures accurate to within a few degrees without computer analysis. Conductive heat transfer is directly proportional to the temperature gradient in the medium. Convective heat transfer is roughly directly proportional to the temperature difference between the material surface and the ambient temperature of the gas. The convection coefficients change slightly as the conditions change, but their variation is small. Therefore, for a system with internal heat generation that is within an ambient gas environment and has no radiative heat transfer, the difference between the temperature at any given location in the system and

the ambient temperature of the gas is almost directly proportional to the heat load. This assumes that the spatial distribution of the heat load does not change, i.e. that the heat generation level at every point moves up and down by the same geometrical factor (or ratio). This is true because the entire spatial temperature profile of the system is expanded or contracted, with all gradients being directly proportional to the heat load.

As an example, consider a DUCRETE cask with "X" times the heat load of the 17.52 kW considered in the ANSYS analyses. The temperatures shown in Table 8 would be modified as follows:

$$T_{\text{new}} = X \cdot (T_{\text{old}} - 100) + 100$$

Since the heat load in the new case is "X" times as much, the amount that each point in the system is over 100°F (the ambient temperature of the environment) is "X" times as great.

This approach is flawed in two respects. First, radiative heat transfer is a highly nonlinear process. As temperatures rise, the radiative heat transfer from a given temperature difference will increase. Second, it does not consider the effects of the solar load, which would produce elevated cask system temperatures (over 100°) without internal heat generation. However, for the cases we are considering, the effects of radiation will not significantly affect the results. The objective is to plot maximum allowable heat load versus allowable DUCRETE temperature. Thus, only the peak DUCRETE temperature, not peak canister temperature, is being considered. Therefore nonlinear radiative heat transfer across the ventilation duct does not bear upon the problem. Also, for the heat transfer across the gap between the DUCRETE cask and the transportation overpack, and for the heat transfer from the cask surface to the external environment, radiation is only responsible for a minor fraction of the total heat transfer.

With respect to the solar heat generation problem, this effect can be accounted for with a simple modification to the formula shown above if, once again, radiation effects are ignored. The overpack surface must not only get rid of the heat generated within the cask, but also the heat generated at the surface due to the solar radiation. One merely needs to calculate the temperature of the overpack surface if the cask internal heat generation were zero, and use that value as the effective ambient temperature in the approximation equation given earlier. Note that with this adjustment the formula will yield the correct overpack surface temperature if the cask internal heat generation is set to zero. Also note that since this temperature will be over the ambient temperature by a small amount, radiation effects will be very small, so they can be ignored without significant loss of accuracy.

Based on the data given in Section 2.1.3, the average solar surface load that is (effectively) applied in the ANSYS models is 23.65 Btu/hr-ft². In the cases where fins are assumed to be present, the effective surface convection coefficient is 2.5 Btu/hr-ft²-°F. This means that with no internal cask heat generation the overpack surface temperature would be about 109.5°F (100 + 23.65/2.5). For the no-fin case, the surface convection coefficient is 0.75 Btu/hr-ft²-°F, so the empty cask surface temperature would be about 131.5°F (100 + 23.65/0.75).

With the additional treatment discussed above, the formula for estimating system temperatures versus heat load for overpacks with fins becomes:

$$T_{\text{new}} = X * (T_{\text{old}} - 109.5) + 109.5$$

and for overpacks without fins:

$$T_{\text{new}} = X * (T_{\text{old}} - 131.5) + 131.5$$

where "X" is defined as the heat load inside the cask exceeding 17.52 kW, the heat source used for the ANSYS results presented in Table 8. The values of T_{old} , for every cask component, are taken from Table 8.

An ANSYS run with the heat load reduced from 17.52 kW all the way down to 6 kW, and other conditions as in Case 1, was performed to verify the accuracy of the temperature estimation formulas given above. This is a stringent test given the large change in cask heat load. This test also spans the heat loads of interest since 6 kW is about as low a heat load as one will find for a 24 PWR element cask, and because the 17.52 kW heat load is almost an upper bound because of the high DUCRETE temperatures it produces. The results shown in Table 9 verify that the simple formulas for estimating temperatures throughout cask systems as a function of cask heat load are accurate to within a few degrees, even though they neglect the nonlinear effects of radiation. Using these formulas, it is a simple matter to plot allowable DUCRETE cask heat load as a function of allowable DUCRETE temperature for each of the cask cases shown in Tables 7 and 8.

4.3.2 DUCRETE Cask Heat Load Limit Results

Using the temperature estimation formulas determined in Section 4.3.1, the peak DUCRETE material temperature is estimated, as a function of heat load, for each of the seven cask cases that were studied with ANSYS. The peak DUCRETE temperatures shown in Table 8 for the seven cases are extrapolated for other heat loads using the estimation formulas. This allows a maximum permissible heat load to be calculated as a function of the maximum allowed DUCRETE temperature. This curve is plotted for the seven cask cases over an allowable DUCRETE temperature range of 200 to 350°F.

The first graph plots allowable heat load vs. allowable DUCRETE temperature for the first four cases described in Table 7. These cases are identical except for the DUCRETE region thermal conductivity. Effective conductivities of 0.72, 1.2, 2.5, and 5.0 Btu/hr-ft-°F were studied. These four

Table 9. Comparison of Calculated and Estimated Peak Cask Component Temperatures for a Low Heat Load Cask (6 kW).

DUCRETE Cask Component	Estimated Temperature (°F)	ANSYS Temperature (°F)
Overpack Surface	125	123
DUCRETE Cask Outer Shell	141	140
DUCRETE Shield	166	164

DUCRETE region conductivities result in four allowable heat load curves, shown in Figure 17. These DUCRETE region conductivities completely span the range of expected values. In a formal design phase, when the DUCRETE region effective thermal conductivity becomes known, the maximum allowable heat load will be able to be found by interpolating between the curves shown in Figure 17.

Cases 5, 6, and 7, as described in Table 7, all have DUCRETE region conductivities of 2.5 Btu/hr-ft-°F. These cases were used to study the effects of removing the overpack fins, filling the cask/overpack gap with water, and electro-polishing the DUCRETE outer shell surface, respectively. The allowable heat load vs. allowable DUCRETE temperature curves for these cases are plotted along with the base case in Figure 18. Comparing each of these curves to the base case curves allows one to clearly see the effects of each of these three system modifications.

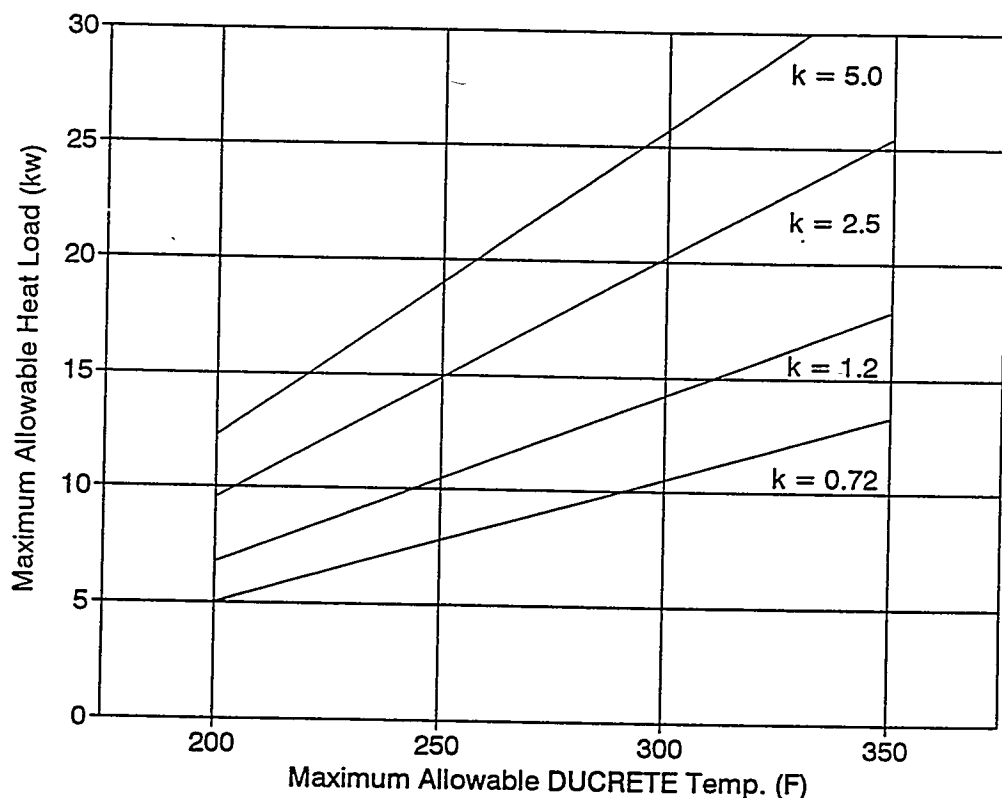


Figure 17. Allowable cask heat load versus maximum allowed DUCRETE temperature for various DUCRETE region thermal conductivities.

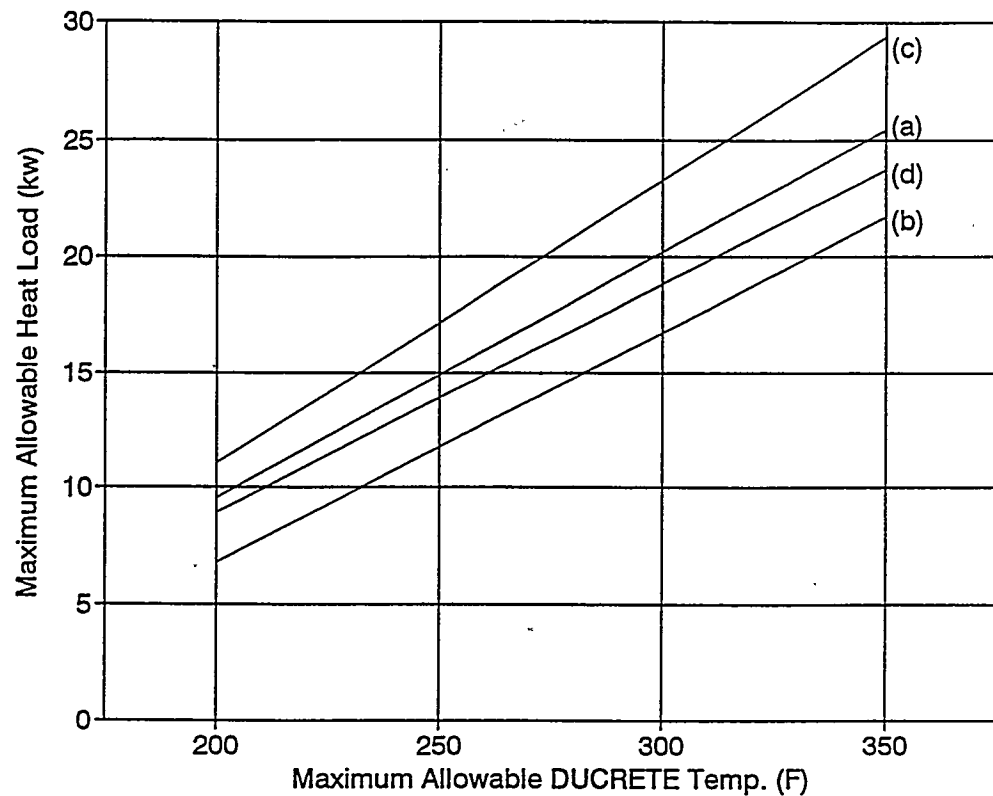


Figure 18. Allowable cask heat load vs. maximum allowed DUCRETE temperature for a) the base case, b) for the no overpack fins case, c) the cask/overpack gap filled with water case, and d) the electro-polished cask outer shell case.

5.0 SHIELDING EVALUATION

As discussed in Section 2, full two-dimensional shielding analyses were performed on the DUCRETE cask inside the transportation overpack using the MCNP code. The MCNP shielding models are illustrated in Figures 4 through 7. Axial peaking of the fuel region gamma and neutron sources were calculated. Gamma dose rate calculations for the cask ends include the contribution from the assembly end fitting sources. The source strengths and axial peaking factors were taken from the MPC system specification.³ The material and geometry description for the MCNP models is given in Section 2.

5.1 Shielding Analyses Performed

Transportation regulations require that the peak total dose rate 2 m from the side of the rail car be no more than 10 mrem/hr. Peak dose rates anywhere on the "package" surface must remain under 200 mrem/hr. The "package" is defined as the transportation overpack and impact limiters. Therefore, the surface dose rate limit for the cask ends applies to the impact limiters, not the end surfaces of the overpack itself. Finally, there is also a 10 mrem/hr limit for 2 m from the front and back ends of the rail car.

Since the rail car dimensions may vary, the shielding analyses conservatively calculate gamma and neutron dose rates 2 m from the overpack surface. Dose rates are also calculated 24 in. from the overpack ends (the impact limiters extend about 24 in. from the cask ends but are not modeled in the shielding analyses) and 2 m away from where the impact limiter surfaces would be (once again assuming no space between the impact limiter ends and the rail car ends).

Neutron dose rates are calculated for the top end of the transportation overpack. The top end surface of the DUCRETE cask is the top lid of the canister. Dose rate calculations for the VSC canister top end have already been performed by Sierra Nuclear.² The MPC canister is expected to produce similar dose rates. Therefore dose rate calculations for the DUCRETE cask (canister) top end were not performed.

Gamma dose rates were not calculated for the overpack top surface because it is obvious that they will be extremely small (under ~1 mrem/hr versus a limit of 200 mrem/hr). This is because the VSC system canister top surface has dose rates that are already less than half the 200 mrem/hr limit, and the transportation overpack adds another 6 in. of solid steel shielding, reducing the dose rate by more than two more orders of magnitude.

Gamma dose rates were also calculated for the bottom end surface of the DUCRETE storage cask. This was done to verify that the DUCRETE cask bottom end shielding is sufficient from perspective of reducing radiation exposures as much as reasonably achievable. Neutron dose rates were not calculated on the DUCRETE cask bottom end. Sierra Nuclear calculations on the SNC canister inside the transfer cask show that neutron dose rates are much smaller than the gamma dose rates.² With the SNC canister inside the transfer cask, there is 9.75 in. of steel shielding on the bottom end (including the canister bottom plate). The total shielding thickness on the DUCRETE cask system bottom end (including the

canister bottom plate) is the same as the VSC system, except that 6 in. of the steel is replaced with DUCRETE. Since DUCRETE is a much better neutron shielding material than steel, neutron dose rates will be significantly lower, making them an even lower fraction of the total bottom end dose rate. Therefore, only gamma dose rates were calculated for the rough estimate of the DUCRETE cask bottom end dose rate. Neutron dose rates were calculated, however, on the bottom end of the transportation overpack.

Finally, a one-dimensional infinite cylinder shielding analysis, like those presented for the storage cask in Reference 1, was performed for the DUCRETE cask geometry described in Section 2.2. This was done to evaluate the effects that the design changes required for transportability have on the DUCRETE cask shielding performance. Also, obtaining surface dose rates for the same cask that is used in the transportation analyses discussed above allows one to determine the dose rate reduction from the transportation overpack. Ratios between storage cask surface dose rates and transportation dose rates can then be established.

5.2 Shielding Analysis Results

The shielding analysis results are summarized in Table 10. The MCNP analyses predict a peak gamma dose rate on the overpack surface of only ~5 mrem/hr, well under the 200 mrem/hr limit. This is true even though the extremely conservative (high) MPC specification gamma source strength and peaking factors are assumed. The gamma dose rates 2 m from the overpack surface are ~1.5 mrem/hr. Neutron dose rates on the overpack surface and 2 m from the overpack surface are 17.5 mrem/hr and 2.5 mrem/hr, respectively. This yields a total dose rate of 22.5 mrem/hr on the overpack side surface, roughly one ninth the limit. The total dose rate 2 m from the overpack surface is ~4 mrem/hr, well under the 10 mrem/hr limit.

Dose rates on the cask system ends are below their limits by an even wider margin. The total dose rate on the overpack bottom surface is about 12 mrem/hr (~5 neutron, ~7 gamma). The dose rate on the bottom surface of the bottom impact limiter is about 8 mrem/hr (~2.5 neutron, ~5.5 gamma). The dose rate 2 m behind the cask package is only ~2 mrem/hr (~0.5 neutron, ~1.5 gamma). There is no dose rate limit for the overpack bottom end. The limit for the bottom impact limiter is 200 mrem/hr, and the limit for 2 m behind the package is 10 mrem/hr. Thus, the dose rates calculated for the systems' bottom end are under their limits by a factor of 5 or more.

The neutron dose rate on the overpack top end is about 16 mrem/hr. Gamma dose rates, as discussed in Section 5.1, are expected to be nil. Neutron dose rates on the top impact limiter surface will be about 8 mrem/hr, and 2 m above this they will be roughly 1 mrem/hr. Thus, on the cask top end, dose rate requirements are met by a factor of ten or more.

MCNP predicts the gamma dose rate on the DUCRETE storage cask bottom end to be ~800 mrem/hr. The neutron dose rate is predicted to be under 50 mrem/hr. The Sierra Nuclear analysis² for the VSC canister and transfer cask yielded a bottom surface neutron dose rate of 80 mrem/hr. The DUCRETE cask bottom end has significantly higher shielding than the VSC system transfer cask since 6 in. of the bottom end steel is replaced with

Table 10. DUCRETE Cask Transportation System Dose Rates (mrem/hr).

Cask System Location	Gamma Dose Rate (mrem/hr)	Neutron Dose Rate (mrem/hr)	Total Dose Rate (mrem/hr)	Dose Rate Limit
2 m from Overpack Side	1.5	2.5	4	10
2 m from Impact Limiter Bottom	1.5	0.5	2	10
2 m from Impact Limiter Top	~0	1	1	10
Overpack Side Surface	5	17.5	22.5	200
Bottom Impact Limiter Surface	5.5	2.5	8	200
Top Impact Limiter Surface	~0	8	8	200
Overpack Bottom Surface	7	5	12	ALARA ^a
Overpack Top Surface	~0	16	16	ALARA
DUCRETE Cask Bottom	~800	~50	~850	ALARA

a. As low as reasonably achievable.

DUCRETE. Therefore, the neutron dose rate is clearly below 50 mrem/hr. This yields a total dose rate estimate of ~850 mrem/hr. There are no regulatory limits on this area of the storage cask surface. While brief contact with this surface is required for decontamination, short exposures to dose rates on the order of 1 rem/hr are commonplace in nuclear plant operations.

To bring cask bottom end dose rates to ~100 mrem/hr, about 3 in. of DUCRETE or 2 in. of steel would have to be added to the DUCRETE cask bottom end. This would increase the DUCRETE cask weight by about 1.75 tons. This is not a problem if a crane capable of lifting over 100 tons is available. If the crane capacity is 100 tons, however, and a maximum weight MPC canister is being used, 1.75 tons of weight would have to be removed from the DUCRETE cask sidewall, increasing sidewall surface dose rates. The expected sidewall dose rate increase would be roughly 25%. Since the cask bottom surface is only very briefly exposed to the outside environment and workers rarely come into contact with it, priority was given to minimizing dose rates on the cask side and top in the design presented in this report.

The one-dimensional storage cask analysis predicts a peak gamma dose rate of 43 mrem/hr and a peak neutron dose rate of 31 mrem/hr on the side surface of the DUCRETE storage cask, based on the dimensions and materials presented in Section 2 of this report and on the MPC Specification source terms for transport mode. If the five-year-cooled (storage mode) source term is assumed, the gamma dose rate becomes 79 mrem/hr and the neutron dose rate becomes 38 mrem/hr, leading to a total peak surface dose rate of 117 mrem/hr. This compares to the ~87 mrem/hr dose rate predicted for the same source in the analyses presented in Reference 1, a 34% increase. Analyses showed that neutron and gamma dose

rates went up by about the same fraction. For the base case VSC source term analyzed in Reference 1, the total dose rate would rise from ~56 mrem/hr to ~75 mrem/hr.

These dose rates are still within the acceptable range, and are within the range that is typical for metal storage casks. The dose rate increase was due to weight that had to be moved from the cask sidewall to the cask bottom to provide additional shielding and structural support. Also, for structural reasons, the DUCRETE cask inner shell had to be made thicker, effectively replacing DUCRETE with an equivalent weight of steel. Steel is a slightly less effective overall radiation shield on a per weight basis. Finally, the new design dimensions allow some weight for an assumed heat transfer fin structure through the DUCRETE material. This required some reduction in the shield region weight. If aluminum fins are used instead of steel, most of this shield weight could be put back. Also, due to the radial orientation of the initially proposed heat transfer fin structure, the shielding analysis took no credit for the steel fin's presence (the steel was modeled as DUCRETE, which has a lower density). If the fin arrangement is not radial (chevron-shaped fins, for example), then more detailed shielding analyses could take credit for the extra heat transfer fin mass in the shield region. These effects will cause the dose rates to move back down towards the values calculated in Reference 1.

5.3 Acceptable Storage Cask Peak Surface Dose Rates

Examining the data shown in Table 10, it can be seen that the 10 mrem/hr dose rate limit 2 m from the side of the overpack is the limiting constraint on the system. If the 43 mrem/hr gamma dose rate on the storage cask surface is compared to the 1.5 mrem/hr gamma dose rate 2 m from the overpack, a reduction factor of about 30 can be determined (the overpack causes about a factor of 9 reduction, and there is another factor of 3 reduction from the distance). Comparing the 31 mrem/hr neutron dose rate on the storage cask side to the 2.5 mrem/hr neutron dose rate 2 m from the overpack yields a reduction factor of ~12 (a factor of 2 from the overpack, and a factor of 6 from distance). Stronger peaking of the neutron source is responsible for the greater fall off rate.

Using these reduction factors, the total dose rate 2 m from the overpack can be estimated from the peak surface dose rates on the storage cask that is about to be transported. The 2 m dose rate will be about 1/30 the peak surface gamma dose rate plus about 1/12 the peak surface neutron dose rate. So, the limit of peak surface dose rate for DUCRETE storage casks about to be shipped is:

$$G/30 + N/12 < 10 \text{ mrem/hr}$$

where G and N are the peak gamma and neutron dose rates (in mrem/hr), respectively, on the storage cask surface.

Another formula can be developed for estimating the dose rates 2 m from the overpack as a function of the peak surface dose rates on the storage cask at the time of loading. This assumes that the fuel has the MPC Specification source terms for storage mode at the time of storage and has the MPC Specification source terms for transport mode at the time of transport. The spectra and axial profiles are assumed to be similar (which they are). The

peak gamma source term at the time of storage is a factor of 1.833 times the source term for transport.³ The peak neutron source for storage is a factor of 1.227 higher than it is for transport. The ratio between the peak surface gamma dose rate at the time of storage and the peak gamma dose rate 2 m from the overpack during transport becomes $\sim 1/55$ ($55 \sim 30 * 1.833$). The neutron ratio becomes $\sim 1/15$ ($15 \sim 12 * 1.227$). This leads to another formula:

$$G_s/55 + N_s/15 < 10 \text{ mrem/hr}$$

where G_s and N_s are the peak surface gamma and neutron dose rates (in mrem/hr), respectively, for the DUCRETE storage cask at the time of storage.

Note that care must be taken when using this second relation, as it assumes that the gamma and neutron dose rates fall between initial storage and transport as do the source strengths specified in the MPC Specification (for storage and transport). This assumption is correct if the fuel is loaded with a cooling time of five years and is shipped with a cooling time of ten years. The formula may fail if the fuel is more than five years old when it is placed in storage because the rate of gamma dose rate decrease between, say, 10 and 15 years is less than it is between five and ten years.

Using the formula above and analyzing the data shown in Reference 1, it appears that the great majority of DUCRETE compositions studied (silica sand as well as colemanite sand) in Reference 1 will produce acceptable dose rates outside the overpack at the time of transport.

6.0 ESTIMATED CASK WEIGHT

As stated in Reference 1, a loaded MPC canister that is filled with water but does not have the structural lid (the top 3 in. of the canister top lid) in place has an estimated weight of ~41 tons. Based upon the geometry described in Section 2.2.1 and shown in Figure 3, and on the material data given in Section 2.2.2, the DUCRETE cask weight is estimated to be roughly 58.2 tons. This includes the weight of the rings that suspend the canister inside the cask cavity (~0.3 tons). Together with the 41 ton canister weight, the DUCRETE storage cask weight is just over 99 tons.

When the system contains a water-filled canister (without the structural lid) it has the maximum weight that the fuel pool crane will have to lift. This is where the 100 ton weight limit applies. A dry canister with the structural lid weighs about 3.5 tons less. In cask loading operations, the water-filled canister, inside the DUCRETE cask, is set down next to the pool. The structural lid is attached and the water is drained before the cask must be lifted again.

This weight assumes no heat transfer fin structure in the DUCRETE material. Fins may add some weight to the cask, depending on the fin material used and the design of the fins. The density of steel is about 50% higher than that of the optimum DUCRETE composition assumed in these analyses. A carbon steel fin structure capable of producing a DUCRETE shield region conductivity of 5 Btu/hr-ft-°F would add more than 1.5 tons to the cask weight. A set of aluminum fins may actually reduce the cask weight.

The DUCRETE cask inlet and outlet vent structure is not yet designed and is not modeled in these analyses. Since the inlet and outlet vents will remove some volume of DUCRETE from the cask (in low dose rate locations), the actual cask will probably be lighter than the model used here. Also, it would be possible to place large chamfers in the DUCRETE cask corners. The depth of the chamfers would be selected so that the peak dose rates in the chamfer region were about equal to the peak dose rates on the cask sidewall near the midplane. This should allow a chamfer about 4 in. deep at the cask corner and reduce cask weight by as much as 2 tons. Given these weight saving effects, which are expected to be incorporated during the formal design phase, we are confident that the total DUCRETE cask weight can be kept under 59 tons, leading to a maximum total loaded cask weight under 100 tons.

The transportation overpack, as shown in Figure 3, weighs about 27.5 tons (including the flared region near the cask top). The aluminum fin design suggested in Section 2.3.2 would add another 1.1 tons to the overpack weight. To allow bonding of the aluminum fins to the stainless steel overpack shell, the shell may have to be coated (clad) with aluminum. A 1/8 in. thick coating of aluminum on the transportation overpack would weigh an additional ~0.3 tons. This leads to a total overpack weight of 28.9 tons.

The DUCRETE cask containing a dry internal canister (with structural lid) weighs about 96.5 tons. Adding this to the overpack weight of 28.9 tons yields a total loaded overpack weight of 125.4 tons, 0.4 tons over the 125 tons transportation cask weight limit. This slight excess at this point in the design effort is very small and is not of concern. The

top and bottom lid thicknesses that are assumed are based on very conservative (and simple) upper bound stress calculations. More detailed analyses performed in the formal design phase will show that thinner lids on the transportation overpack will be sufficient. They will also be more than sufficient from a shielding perspective. Furthermore, as mentioned earlier, the DUCRETE cask may end up weighing less than 59 tons and the loaded canister may weigh less than 37.5 tons. The above calculation assumed the maximum allowable storage cask weight of 96.5 tons (after water drainage).

As mentioned in Section 2.3.3, the estimated weight of the transportation system impact limiters is about 7 tons. The 125 ton weight limit does not include impact limiter weight, however. The weight of the entire package when it is on the rail car will be ~132 tons.

Some reduction, from the initial storage cask design, in the weight of the DUCRETE cask sidewall was necessary to allow the cask to be transportable. The steel cask components had to be made thicker to meet transportation structural criteria, especially the cask bottom end plates. This made the bottom end structure of the cask somewhat heavier, requiring some weight to be pulled from the cask sidewall. Also, about one ton of weight was reserved for a heat transfer fin structure. As a result, although the total DUCRETE cask wall thickness is 11 in. (the thickness that, according to Reference 1, corresponds to DUCRETE with a UO₂ volume fraction of 50%), the DUCRETE mixture that is assumed has a UO₂ volume fraction of only 45%. This does lead to somewhat higher peak surface dose rates for the DUCRETE storage cask, as discussed in Section 5.

7.0 CONCLUSIONS

Structural, thermal, and shielding calculations have been performed on the DUCRETE cask transportation system. This system consists of the DUCRETE storage cask, described in Reference 1 and in Section 1.2 of this report, and a simple steel transportation overpack. The overpack forms the containment boundary of the DUCRETE cask system and is the main structural component with respect to transportation structural requirements. Thus, the transportation overpack greatly reduces the structural requirements on the DUCRETE cask, which minimizes the cost of the DUCRETE storage cask. This greatly affects overall system economics since the DUCRETE storage cask must be produced in large numbers. The overpack also provides substantial additional shielding. Unfortunately, when the storage casks are placed within the overpack, the storage cask internal ventilation is cut off and the ventilation duct becomes an insulating dead air (or helium) space.

Conservative manual calculations verify the adequacy of the transportation overpack with respect to transportation structural requirements. One structural issue specific to the DUCRETE cask system concerns the ventilation duct in the DUCRETE storage cask. When the storage cask is placed in a horizontal position, a mechanism must be found to suspend the inner canister near the center of the much larger DUCRETE cask cavity. The analyses showed that if the canister is suspended by its ends by two steel rings (which form the top and bottom boundaries of the ventilation duct) it can withstand the bending stresses associated with a 30 foot side drop event.

Two-dimensional computational shielding analyses, using the MCNP shielding code, were performed for the DUCRETE cask transportation system. The analyses show that the DUCRETE transportation system yields dose rates (outside the overpack) that are well under transportation dose rate limits even if the very high source strengths that are specified for the DOE MPC canister are assumed.

An explicit two-dimensional finite difference model of the DUCRETE cask inside the overpack was developed. Thermal analyses were performed using the ANSYS code. The ventilation duct was modeled as a dead space with no internal convection. The thermal conductivity of DUCRETE is not yet known, so a wide range of thermal conductivities for the DUCRETE shield region were studied, including some cases that assume the presence of a heat transfer fin structure through the DUCRETE. Other features, such as surface fins on the overpack and putting water in the gap between the DUCRETE cask and the overpack, were also studied. The analyses modeled the axial heat source distribution in the fuel and the effects of solar radiation on the cask.

The results of the thermal analyses were allowable cask heat sources as a function of the allowable DUCRETE temperature and DUCRETE region conductivity. The maximum allowable temperature for DUCRETE is not yet known. The thermal analyses showed that the maximum allowable DUCRETE temperature will limit the thermal performance of the system. Fuel cladding temperature limits will not be a concern.

The results also show that, unless the short term temperature limit for DUCRETE turns out to be higher than expected (over 300°F), heat transfer fins through the DUCRETE shield

will be required to accommodate canister heat loads of 16 kW or more. This is the heat load range that is expected for 24 PWR assemblies with a 10 year cooling time and a burnup level of ~35,000 MWd/MTU. With a maximum allowable DUCRETE temperature that is under 300°F, the heat load that could be accommodated without fins is at most 12-14 kW. In addition, for reasonable thermal performance, an extensive array of heat transfer fins will probably be required on the overpack outer surface. Even with a fin structure through the DUCRETE shield, the heat load will probably be limited to under 15 kW, if no fin structure is present on the overpack surface.

Weight calculations showed that the weight of a loaded canister (with water weight) inside a DUCRETE storage cask will be under 100 tons, meeting the MPC specification weight limit for loaded on-site storage casks. Also, the total weight of the overpack with a loaded DUCRETE cask and (dry) loaded canister is shown to be ~125 tons, meeting the MPC system specification for a loaded transport cask.

8.0 REFERENCES

1. J. E. Hopf, *Conceptual Design Report for the DUCRETE Spent Fuel Storage Cask System*, INEL-95/0030, Idaho National Engineering Laboratory, February 1995.
2. *Safety Analysis Report for the Ventilated Storage Cask System*, SNC-94-001, October 1994 Revision.
3. Multi-Purpose Canister (MPC) Subsystem Design Procurement Specification, Revision 4, DBG000000-01717-6300-00001 REV 4, August 26, 1994.
4. OCRWM/ORNL Spent Fuel Photon and Neutron PC Database System, Waste Characterization Task Group, Oak Ridge National Laboratory, December 1986.
5. F. P. Incropera and D. P. DeWitt, *Fundamentals of Heat and Mass Transfer*, Second Ed., John Wiley & Sons, 1985.
6. B. Sappert, *A Guide for Design, Fabrication and Operation of Shipping Casks for Nuclear Applications*, Oak Ridge National Laboratory, February 1970.
7. R. J. Roark, *Formulas for Stress and Strain*, Fourth Ed., McGraw-Hill, 1965.
8. F. Merritt, *Standard Handbook for Civil Engineers*, Third Ed., McGraw-Hill, 1983.